

Integrative taxonomic and geographic variation analyses in *Cyrtodactylus aequalis* (Squamata: Gekkonidae) from southern Myanmar (Burma): one species, two different stories

L. Lee Grismer^{a,*}, Perry L. Wood Jr.^b, Marta S. Grismer^a, Evan S.H. Quah^{a,c}, Myint Kyaw Thura^d, Jamie R. Oaks^b, Aung Lin^e and Diana Y. Lim^a

^aHerpetology Laboratory, Department of Biology, La Sierra University, 4500 Riverwalk Parkway, Riverside, California 92515, USA

^bDepartment of Biological Sciences & Museum of Natural History, Auburn University, Auburn, Alabama 36849, USA

^cInstitute of Tropical Biodiversity and Sustainable Development, Universiti Malaysia Terengganu, 21030 Kuala Terengganu, Terengganu, Malaysia

^dMyanmar Environment Sustainable Conservation, Yangon, Myanmar

^eFauna and Flora International, No(35), 3rd Floor, Shan Gone Condo, Myay Ni Gone Market Street, Sanchaung Township, Yangon, Myanmar

Abstract The historical accuracy of building taxonomies is improved when they are based on phylogenetic inference (i.e., the resultant classifications are less apt to misrepresent evolutionary history). In fact, taxonomies inferred from statistically significant diagnostic morphological characters in the absence of phylogenetic considerations, can contain non-monophyletic lineages. This is especially true at the species level where small amounts of gene flow may not preclude the evolution of localized adaptations in different geographic areas while underpinning the paraphyletic nature of each population with respect to the other. We illustrate this point by examining genetic and morphological variation among three putatively allopatric populations of the granite-dwelling Bent-toed Gecko *Cyrtodactylus aequalis* from hilly regions in southeastern Myanmar. In the absence of molecular phylogenetic inference, a compelling argument for three morphologically diagnosable species could be marshaled. However, when basing the morphological analyses of geographic variation on a molecular phylogeny, there is a more compelling argument that only one species should be recognized. We are cognizant of the fact however, that when dealing with rare species or specimens for which no molecular data are possible, judicious morphological analyses are the only option—and the desired option given the current worldwide biodiversity crisis.

Keywords Taxonomy; phylogeny; phylogeography; Gekkonidae; Asia; conservation

Introduction

Taxonomy—the description and naming of species—has become increasingly more sophisticated and exacting within the context of integrative frameworks (Aherns et al., 2013; Hu et al., 2019; Mathews et al., 2008; Padial et al., 2010; Slater et al., 2013). This is especially true with the incorporation of judiciously used genetic data which can couple species delimitation with phylogeny (e.g., Pons et al., 2006; Sukumaran and Knowles, 2017; Schield et al., 2018; Watson et al., 2019), thus eliminating a myriad of phyletic problems when trying to delimit species using only traditional taxonomic methods based solely on morphology (Watson et al., 2019). Furthermore, integrative analyses can be used to identify weakly divergent clades bearing significant phenotypic differentiation (or the reverse) and to assess early stages of speciation (Hu et al., 2019). Nonetheless, morphology remains a critical component of taxonomy and the types of analyses performed on morphological data bear on the taxonomic interpretation of the outcome. This is especially true when examining multiple populations that may or may not be conspecific, may or may not be allopatric, and show only limited amounts of intra- or interpopulation genetic variation. Under these

circumstances, which are the appropriate integrative analytical tools to delimit putative species and what does one do when the analyses do not necessarily agree? We explore some of these issues in a species of Bent-toed Gecko (*Cyrtodactylus aequalis*) endemic to southeastern Myanmar.

In recent years, *Cyrtodactylus* Gray has rapidly become the most species rich lizard genus in Myanmar with the description of 28 new species in just under two years (Connette et al., 2017; Grismer et al., 2018a, b, c, d, e, f; Grismer et al., 2019a, b, 2020). One species, *C. aequalis* was described on the basis of a single specimen from the base of Kyaiktiyo Mountain in Mon State at 382 m in elevation (Bauer, 2003). However, the phylogenetic relationships and life history of *C. aequalis* remained unknown until Grismer et al. (2018a) reported on a second specimen taken from within the crack of a granite boulder on the top of Kyaiktiyo Mountain at 1057 m in elevation (Fig. 1) and placed it within what they designated as the *C. sinyineensis* group—a clade of karst-associated species largely endemic to the low-lying Salween Basin in Kayin and Mon states. Their most recent molecular phylogeny (Grismer et al., 2019c), recovered *C. aequalis* as most closely related to the karst-dwelling sister species *C. bayinnyiensis* and

*Corresponding author. E-mail: lgrismer@lasierra.edu

C. dattkyaikensis. In that report, Grismer et al. (2020) reported on a series of 15 additional specimens of *C. aequalis* from the same upland granitic region that included juveniles and a gravid female with a SVL of 87.1 mm. They also reported on four additional specimens from a newly discovered population 28 km to the south at Kay Lar Tha—a granitic hill reaching 350 m in elevation isolated in an agricultural flood plain at the head of the Gulf of Martaban (Fig. 1). All four specimens were collected among granite boulders and one was a gravid female with an SVL of 68.0 mm. The specimens of this population composed the reciprocally monophyletic sister lineage to the Kyaiktiyo Mountain population but with only a 0.01% uncorrected pairwise sequence divergence between them even though they had significantly different mean values in a number of morphological characters (Grismer et al., 2020). Based on these data, Grismer et al. (2020) refrained from formally recognizing the Kay Lar Tha population as a distinct species, referring to it as *C. cf. aequalis*, and noting that any formal taxonomic recognition could not be properly evaluated in the absence of additional samples from intervening geographic areas.

We recently traveled to Kou Thi Nar Youn, an upland granite area 23 km southeast of Kyaiktiyo and 16 km north of Kay Lar Tha reaching 307 m in elevation (Fig. 1). We collected a series of 11 specimens among granitic boulders including a gravid female with an SVL of 78.4 mm. We also examined seven additional specimens of *C. aequalis* from the vicinity of the type locality at the base of Kyaiktiyo Mountain from between 49 m and 395 m in elevation. Herein, we examine the phylogeographic structure among the three populations using the mitochondrial gene NADH dehydrogenase subunit 2 (ND2) and its flanking tRNA regions. Independent of their phylogeographic structure, we examined geographic variation among the three populations using a battery of comparative multivariate and univariate statistical analyses on meristic (sculptation) and mensural (morphometrics) data sets. We compare and discuss the results of these analyses and their taxonomic implications.

Materials and methods

Species delimitation

The general lineage concept (GLC; de Queiroz, 2007) adopted herein proposes that a species constitutes a population of organisms evolving independently from other such populations owing to a lack of gene flow. By “independently,” it is meant that new mutations arising in one species cannot spread readily into another species (Barraclough et al., 2003; de Queiroz, 2007). Integrative studies on the nature and origins of species are using an increasingly wider range of empirical data to delimit species boundaries (Coyne and Orr, 1998; Fontaneto et al., 2007; Knowles and Carstens, 2007; Leaché et al., 2009), rather than relying solely on morphology and traditional taxonomic methods. Under the GLC implemented herein, molecular phylogenies were used to recover monophyletic mitochondrial lineages of individuals (populations)

in order to develop initial species-level hypotheses—the grouping stage of Hillis (2019). Discrete color pattern characters and univariate and multivariate analyses of morphological data were then used to search for characters and morphospacial patterns bearing statistically significant differences that were consistent with the phylogeny-based species-level hypotheses—the construction of boundaries representing the hypothesis-testing step of Hillis (2019)—thus providing independent diagnoses to complement the molecular analyses. Species boundaries were subsequently cross-checked using a Generalized Mixed Yule Coalescent (GMYC) approach (Pons et al., 2006), thus providing an additional framework to complement the empirically based hypotheses of the morphological and molecular analyses.

Molecular data and analyses

The primary aim of this study was to investigate the taxonomic implications of the phylogeographic structure and geographic variation among the three populations of *Cyrtodactylus aequalis* based on 1482 bp of ND2 and its flanking tRNAs (WANCY region) and meristic and mensural morphological data. The molecular data set of Grismer et al. (2020), which included exemplars of all the major *Cyrtodactylus* clades in Wood et al. (2012) and Agarwal et al. (2014) and all species of the *C. sinyineensis* group to which *C. aequalis* belongs, was augmented with 11 samples from Kou Thi Nar Youn totaling 330 ingroup samples. *Hemidactylus angulatus*, *H. frenatus*, *H. garnotii*, *H. mabouia*, and *H. turcicus* served as outgroups following Wood et al. (2012) and Grismer et al. (2019c). The new *C. aequalis* sequences were deposited in GenBank (Table 1).

Genomic DNA was isolated from liver or skeletal muscle specimens stored in 95% ethanol using a SPRI magnetic bead extraction protocol (<https://github.com/phyleticalab-protocols/blob/master/extraction-spri.md>). The ND2 gene was amplified using a double-stranded Polymerase Chain Reaction (PCR) under the following conditions: 1.0 µl genomic DNA (10–30 µg), 1.0 µl light strand primer (concentration 10 µM), 1.0 µl heavy strand primer (concentration 10 µM), 1.0 µl dinucleotide pairs (1.5 µM), 2.0 µl 5x buffer (1.5 µM), MgCl 10x buffer (1.5 µM), 0.1 µl Taq polymerase (5u/µl), and 6.4 µl ultra-pure H₂O. PCR reactions were executed on Bio-Rad gradient thermocycler under the following conditions: initial denaturation at 95°C for 2 min, followed by a second denaturation at 95°C for 35 s, annealing at 55°C for 35 s, followed by a cycle extension at 72°C for 35 s, for 31 cycles. All PCR products were visualized on a 1.0 % agarose gel electrophoresis. Successful PCR products were sent to GENEWIZ® for PCR purification, cycle sequencing, sequencing purification, and sequencing using the same primers as in the amplification step (Table 2). Sequences were analyzed from both the 3' and the 5' ends separately to confirm congruence between reads. Forward and reverse sequences were uploaded and edited in Geneious™ 2019.0.4 (<https://www.geneious.com>). Following sequence editing we aligned the protein-coding region and the flanking tRNAs using

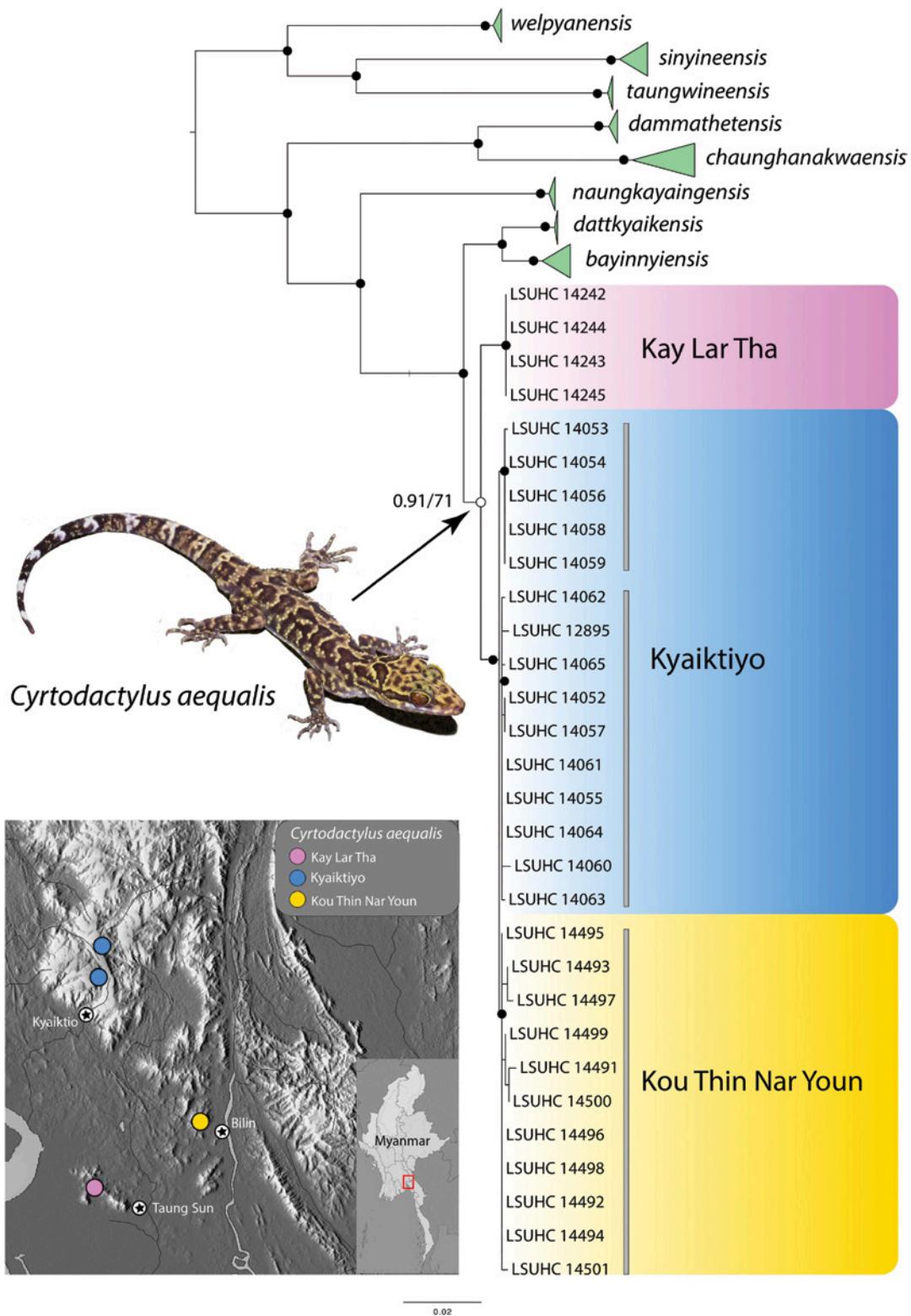


Figure 1. Maximum likelihood consensus tree of the *Cyrtodactylus sinyineensis* group with 1.00 and 100 BI and UFB support values, respectively, at the nodes designated by black circles. The gray vertical bars delimit three lineages of a polytomy. Map showing the localities of the three areas where the populations of *C. aequalis* are located.

the MAFFT v7.017 (Kato and Kuma, 2002) plugin under the default settings in Geneious™ 2019.0.4 (<https://www.geneious.com>). Mesquite v3.04 (Maddison and Maddison, 2015) was used to calculate the correct amino acid reading frame and to confirm the lack of premature stop codons in the ND2 portion of the DNA fragment.

We used both maximum likelihood (ML) and Bayesian inference (BI) to estimate the phylogenetic relationships among the sampled geckos in our sequence alignment. An ML phylogeny was estimated in the W-IQ-TREE webserver (Nguyen et al., 2015; Trifinopoulos et al., 2016) preceded by the selection of a substitution

Table 1. GenBank accession numbers for the newly recorded specimens of *Cyrtodactylus aequalis* used in the molecular phylogenetic analyses based on ND2. Accession numbers for outgroups are in Agarwal et al. (2014) and for the other species of the *Cyrtodactylus sinyineensis* group see Grismer et al. (2019c).

Taxon	Catalog no.	Locality	GenBank no.
<i>Cyrtodactylus aequalis</i>	LSUHC 14491	Kou Thi Nar Youn, Mon State, Myanmar (N 17.29775, E 97.21665)	MN917682
<i>Cyrtodactylus aequalis</i>	LSUHC 14492	Kou Thi Nar Youn, Mon State, Myanmar (N 17.29775, E 97.21665)	MN917683
<i>Cyrtodactylus aequalis</i>	LSUHC 14493	Kou Thi Nar Youn, Mon State, Myanmar (N 17.29775, E 97.21665)	MN917684
<i>Cyrtodactylus aequalis</i>	LSUHC 14494	Kou Thi Nar Youn, Mon State, Myanmar (N 17.29775, E 97.21665)	MN917685
<i>Cyrtodactylus aequalis</i>	LSUHC 14495	Kou Thi Nar Youn, Mon State, Myanmar (N 17.29775, E 97.21665)	MN917686
<i>Cyrtodactylus aequalis</i>	LSUHC 14496	Kou Thi Nar Youn, Mon State, Myanmar (N 17.29775, E 97.21665)	MN917687
<i>Cyrtodactylus aequalis</i>	LSUHC 14497	Kou Thi Nar Youn, Mon State, Myanmar (N 17.29775, E 97.21665)	MN917688
<i>Cyrtodactylus aequalis</i>	LSUHC 14498	Kou Thi Nar Youn, Mon State, Myanmar (N 17.29775, E 97.21665)	MN917689
<i>Cyrtodactylus aequalis</i>	LSUHC 14499	Kou Thi Nar Youn, Mon State, Myanmar (N 17.29775, E 97.21665)	MN917690
<i>Cyrtodactylus aequalis</i>	LSUHC 14500	Kou Thi Nar Youn, Mon State, Myanmar (N 17.29775, E 97.21665)	MN917691
<i>Cyrtodactylus aequalis</i>	LSUHC 14501	Kou Thi Nar Youn, Mon State, Myanmar (N 17.29775, E 97.21665)	MN917692

Table 2. Primer sequences used for amplification and sequencing of the ND2 gene and the flanking tRNAs.

Primer name	Primer reference		Sequence
L4437b	(Macey et al., 1997)	External	5'-AAGCAGTTGGGCCCATACC-3'
H5934	(Macey et al., 1997)	External	5'-AGRGTGCCAATGTCTTTGTGRTT-3'

model using the Bayesian Information Criterion (BIC) in ModelFinder (Kalyaanamoorthy et al., 2017), which supported K2P+I+ Γ 4 as the best fit model of evolution for the tRNAs and HKY+F+ Γ 4 for ND2 codon position one, HKY+F+I for position 2, and TIM2+F for position 3. One-thousand bootstrap pseudoreplicates via the ultrafast bootstrap (UFB; Hoang et al., 2018) approximation algorithm were employed and nodes having ML UFB values of 95 and above were considered highly supported (Minh et al., 2013). A Bayesian inference (BI) phylogenetic analysis was carried out in MrBayes 3.2.3. on XSEDE (Ronquist et al., 2012) through the CIPRES Science Gateway (Cyberinfrastructure for Phylogenetic Research; Miller et al., 2010) employing default priors and models of evolution that most closely approximated those in the ML analysis: K2P+I+ Γ 4 for the tRNAs and HKY+ Γ for ND2 codon position one and HKY+I for positions 2 and 3. Two independent Markov chain Monte Carlo (MCMC) analyses were performed each with four chains, three hot and one cold. We ran the MCMC simulation for 150 million generations, sampled every 15 thousand generations and discarded the first 25% of each run as burn-in. Convergence and stationarity of all parameters from both runs were checked in Tracer v1.6 (Rambaut et al., 2014) to ensure effective sample sizes (ESS) were above 200. Post-burn-in sampled trees from both runs were combined and a 50% majority-rule consensus tree was constructed. Nodes with Bayesian posterior probabilities of 0.95 and above were considered highly supported (Huelsenbeck et al., 2001; Wilcox et al., 2002). After removing outgroup taxa, MEGA7 (Kumar et al., 2016) was used to calculate uncorrected pairwise sequence divergence among the individuals of *C. aequalis*.

An ultrametric tree was estimated using in BEAST v2.4.6 (Bayesian Evolutionary Analysis Sampling Trees; Drummond et al., 2012) and was used to perform the

Generalized Mixed Yule Coalescent (GMYC) approach to species delimitation (Pons et al., 2006). The settings of the BEAST analysis were configured in BEAUti version v2.4.7 (Bayesian Evolutionary Analysis Utility) and run with BEAST v2.4.6 on CIPRES employing a lognormal relaxed clock with separate (unlinked) substitution and clock models for the tRNAs and the three codon positions of ND2. Uncertainty in the model of evolution for each partition was averaged over during phylogenetic inference using bModelTest. MCMC chains were run using a coalescent exponential population prior for 150,000,000 million generations and logged every 15,000 generations. The BEAST log file was visualized and checked in Tracer v1.6.0 (Rambaut et al., 2014) to ensure ESS values were above 200 for all parameters. A maximum clade credibility tree using mean heights at the nodes was generated using TreeAnnotator v1.8.0 (Rambaut and Drummond, 2013) with a burnin of 1000 trees (10%).

The Generalized Mixed Yule Coalescent (GMYC) approach is a method for delimiting species from single-locus, ultrametric gene trees by detecting genetic clustering beyond the expected levels of a null hypothesis which infers that all individuals of a population form a genetically interacting nexus. In clades where effective population sizes are not necessarily low and divergence times among the populations are not high, the multi-threshold version of the model (such as that used herein) outperforms the single-threshold version (Fujisawa and Barraclough, 2013). The GMYC relies on the prediction that independent evolution leads to the appearance of distinct genetic clusters, separated by relatively longer internal branches (Barraclough et al., 2003; Acinas et al., 2004). Such groups therefore, diverge into discrete units of morphological and genetic variation that are recovered with surveys of higher clades. The analysis was run on a web server at <http://species.h-its.org/gmyc/> on 1 October 2019.

Morphological data and analyses

Character descriptions

Color notes and digital images were taken from living specimens of the three populations of *Cyrtodactylus aequalis* prior to preservation. Measurements were taken on the left side of the body when possible to the nearest 0.1 mm using Mitutoyo dial calipers under a Nikon SMZ 1500 dissecting microscope. Measurements following Grismer and Grismer (2017) and Grismer et al. (2018a, b) were: snout-vent length (SVL), taken from the tip of snout to the vent; head length (HL), the distance from the posterior margin of the retroarticular process of the lower jaw to the tip of the snout; head width (HW), measured at the angle of the jaws; head depth (HD), the maximum height of head posterior to the eyes measured from the occiput to the ventral margins of the mandibles; eye diameter (ED), the greatest horizontal diameter of the eye-ball; snout length (SNT), measured from anteriormost margin of the boney orbit to the tip of snout; pelvic width (PW), distance between the lateral edges of the dorsal tips of the ilia; pelvic height (PH), distance from the dorsal tip of an ilium to the ventral surface of the pubis; forelimb width (FLW), measured from the anterior to the posterior margins of a brachium immediately adjacent to its insertion points on the body; and forelimb length (FLL), measured from a point equidistant between its anterior and posterior insertion points on the body to the tip of the fourth finger; hind limb width (HLW), measured from the anterior to the posterior margins of a thigh immediately adjacent to its insertion points on the body; hind limb length (HLL), measured from a point equidistant between its anterior and posterior insertion points on the body to the tip of the fourth toe; and axilla to groin length (AG), taken from the posterior margin of the forelimb at its insertion point on the body to the anterior margin of the hind limb at its insertion point on the body.

Meristic characters following Grismer et al. (2020) taken were the numbers of supralabial scales (SL) counted from the largest scale immediately below the middle of the eyeball to the rostral scale and infralabial scales (IL), the large scales counted from the mental scale to the commissure of the jaw; number of paravertebral tubercles (PV) between limb insertions counted in a straight line immediately left and right of the vertebral column and averaged; the number of longitudinal rows of body tubercles (LT) counted transversely across the center of the dorsum from one ventrolateral fold to the other; the number of longitudinal rows of ventral scales (VS) counted transversely across the center of the abdomen from one ventrolateral fold to the other; the number of expanded subdigital lamellae proximal to the digital inflection on the fourth toe (ETL) counted from the base of the first phalanx where it contacts the body of the foot to the largest scale on the digital inflection (see Grismer et al., 2018a: Fig. 3; the large continuous scales on the palmar and plantar surfaces were not counted); the number of small, unmodified subdigital lamellae distal to the digital inflection on the fourth toe (UTL) counted from the digital inflection to the claw (see Grismer et al., 2018a: Fig. 3); and the total number of subdigital lamellae (TTL) beneath the fourth toe

(i.e., $ETL + UTL = TTL$). The total number of enlarged femoral scales (FS) from each thigh were combined as a single metric. The total number of femoral pores (FP) in males (i.e., the sum of the number of enlarged pore-bearing femoral scales from each leg combined as a single metric (n.b. not all enlarged femoral scales have pores). The number of enlarged precloacal scales (PS); the number of precloacal pores in (PP) in males; the number of rows of large post-precloacal scales (PPS) on the midline between the enlarged precloacal scales and the vent (see Grismer et al., 2018a: Fig. 4); and estimate of number of dark body bands (BB) between the occiput and the hind limb insertions not including the sacral or postsacral bands (the irregularly shaped bands in some specimens precludes an accurate count); the number of light-colored caudal bands on an original tail; the number of dark caudal bands on an original tail; and if a mature regenerated tail was spotted or not.

Non-meristic morphological characters evaluated were the degree of body tuberculation—weak tuberculation referring to dorsal body tubercles that are relatively low, small, less densely packed, and weakly keeled whereas prominent tuberculation refers to tubercles that are larger, higher (raised), and prominently keeled (see Grismer et al., 2018a: Fig. 6); body tubercles extending past the postcloacal swelling or not (see Grismer et al., 2018a: Fig. 7); and the relative length-to-width ratio of the transversely expanded, median subcaudal scales and whether or not they extend onto the lateral surface of the tail (see Grismer et al., 2018a: Fig. 8).

Color pattern characters (see Grismer et al., 2018a: Fig. 5) evaluated were the nuchal loop being continuous from eye to eye, separated medially into paravertebral halves, bearing an anterior azygous notch or not, and the posterior border being straight (smooth), sinuous, v-shaped, jagged, or having two posteriorly directed projections; dorsal body bands bearing paired, paravertebral elements or not; dark dorsal body bands wider than light interspaces, with or without lightened centers, edged with light-colored tubercles or not, jagged or more regularly shaped (straight or even-edged); dark markings present or absent in the dorsal interspaces; top of head bearing combinations of dark diffuse mottling or dark, distinct blotches overlain with a light-colored reticulating network or not; light caudal bands bearing dark markings or immaculate; light caudal bands encircle tail or not; dark caudal bands wider than light caudal bands or not; and regenerated tail bearing a pattern of distinct, dark spots or not.

Integrative analysis

The morphological data were used in two separate analyses. The first analysis was completely integrative in that the morphological data were evaluated on the basis of tree topology where monophyletic mitochondrial lineages were considered putative species and composed the operational taxonomic units (OTUs) of the analyses. Various statistical analyses (see below) of these data were employed to ascertain if the different mitochondrial lineages corresponded to populations bearing statistically different morphological

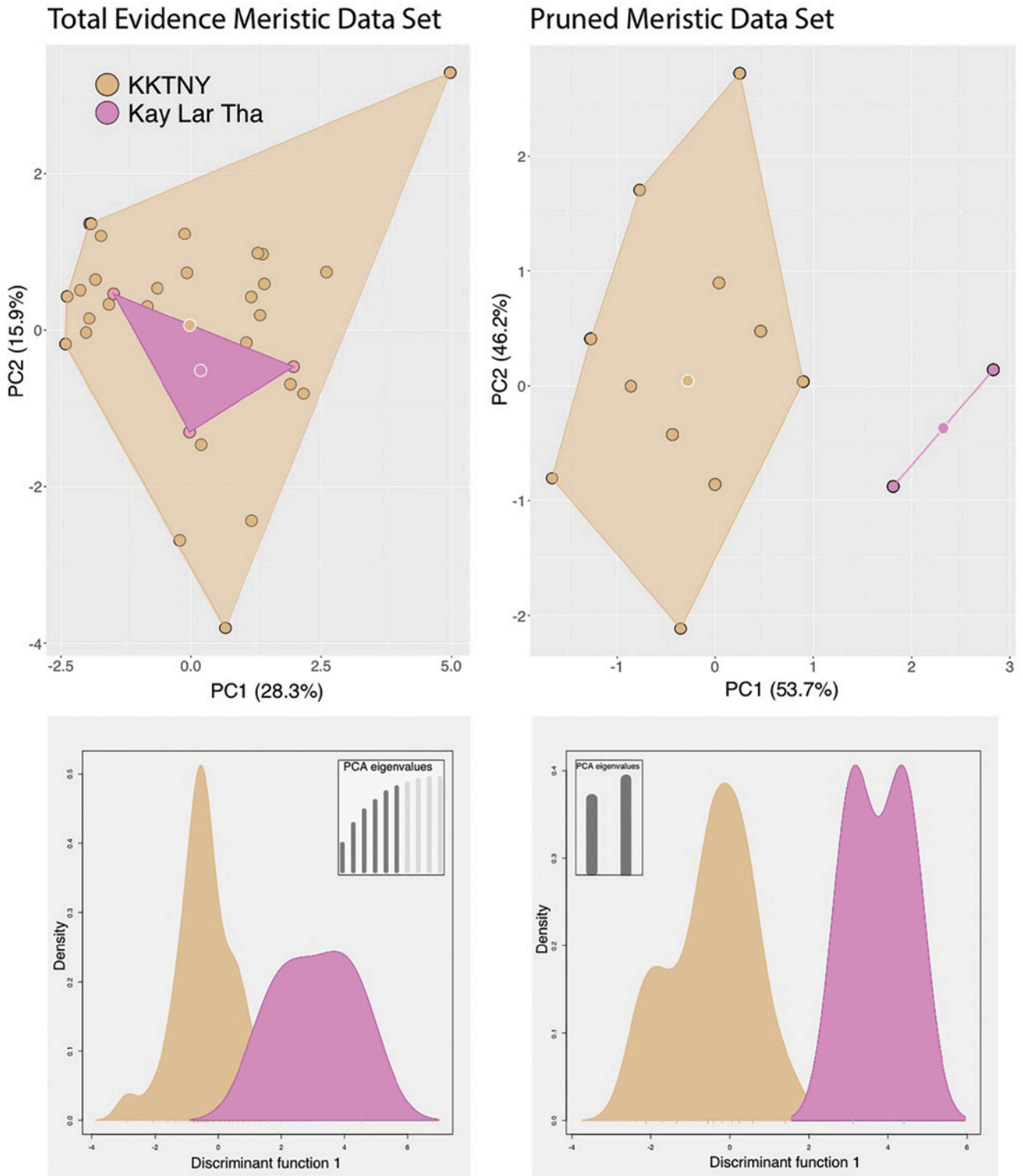


Figure 2. PCA and DAPC discriminant function plots of the total evidence and pruned meristic data sets from the integrative taxonomic analysis. KKTNY = the combined metrics for the Kyaiktiyo and Kou Thi Nar Youn populations.

characteristics. For this analysis, the Kyaiktiyo and Kou Thi Nar Youn samples were combined into a single OTU (KKTNY) owing to their polytomic relationship (see below). KKTNY was compared only to the Kay Lar Tha population.

Geographic variation analyses

The second analysis assessed geographic variation across the three populations of *Cyrtodactylus aequalis* regardless

of the phylogenetic substructuring of its individuals. Individuals from each of the three locations were treated as distinct OTUs and compared to one another using various statistical models (see below).

Statistical analyses of morphology

All statistical analyses were performed using the platform R v 3.2.1 (R Core Team, 2018). For both the integrative and geographic variation analyses, separate analyses of

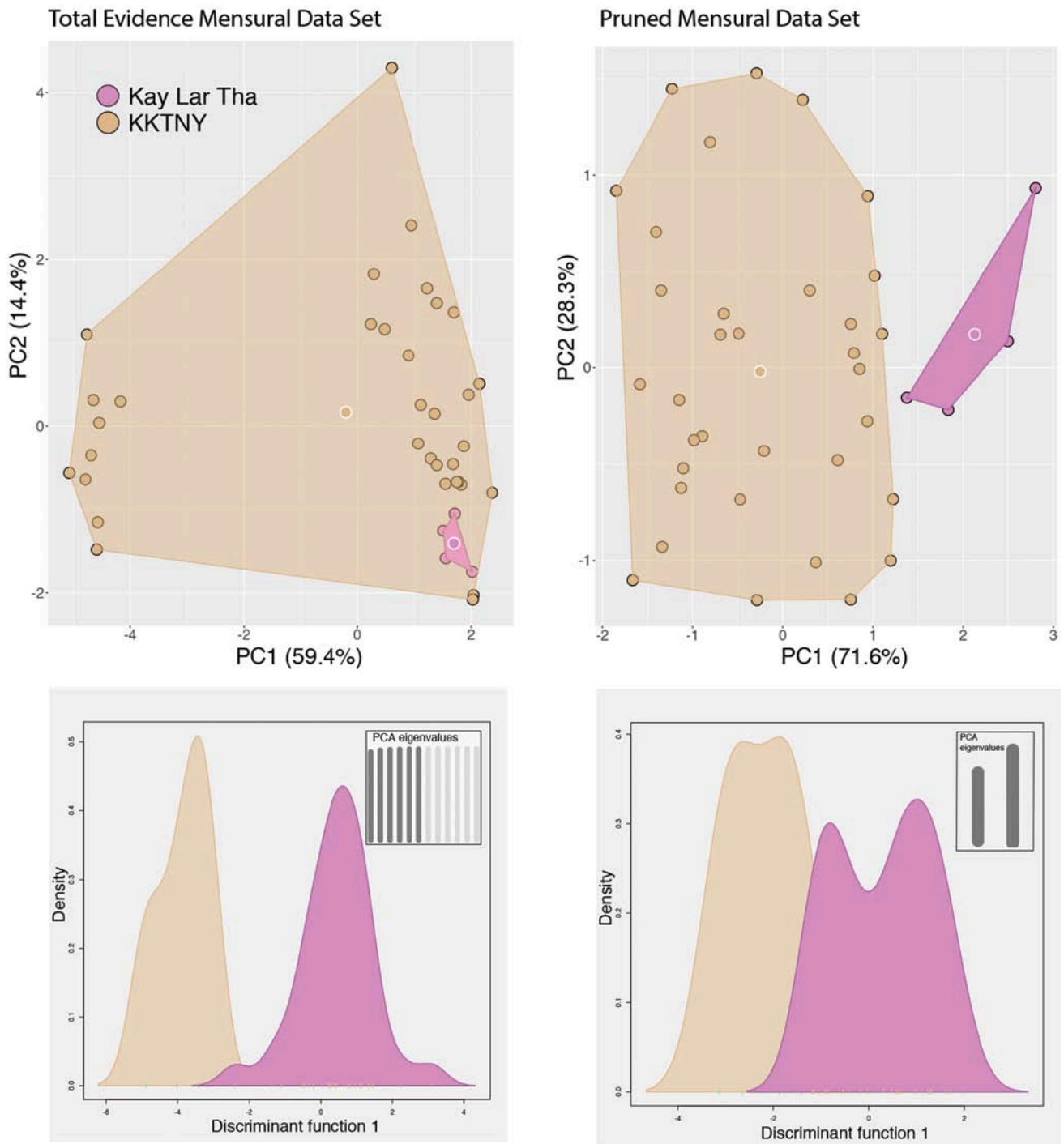


Figure 3. PCA and DAPC discriminant function plots of the total evidence and pruned mensural data sets from the integrative taxonomic analysis. KKTNY = the combined metrics for the Kyaiktiyo and Kou Thi Nar Youn populations.

variance (ANOVA) were conducted on meristic and mensural characters with similar variances (i.e., $p \geq 0.05$ in a Levene's test) to test for the presence of statistically significant mean differences ($p \leq 0.05$) in their data sets. Characters bearing statistical differences within the data set were subjected to a TukeyHSD test to ascertain which OTU pairs differed significantly from each other for those particular characters. Histograms and ridge plots were generated using a custom R script in order to visualize the range of variation and the degree of differences between pairs of OTUs bearing significantly different means.

For both the integrative and geographic variation analyses, morphospacial positions were subsequently compared using principal component analysis (PCA) from the ADEGENET package in R (Jombart et al., 2010) to determine if their positioning was consistent with the putative species boundaries delimited by the molecular phylogenetic analyses (in the case of the integrative analysis only) and defined by the univariate analyses. PCA is a dimension reducing algorithm that decreases the complexity of a data set by finding a subset of input variables that contain the most relevant information (i.e., the most variance in the data)

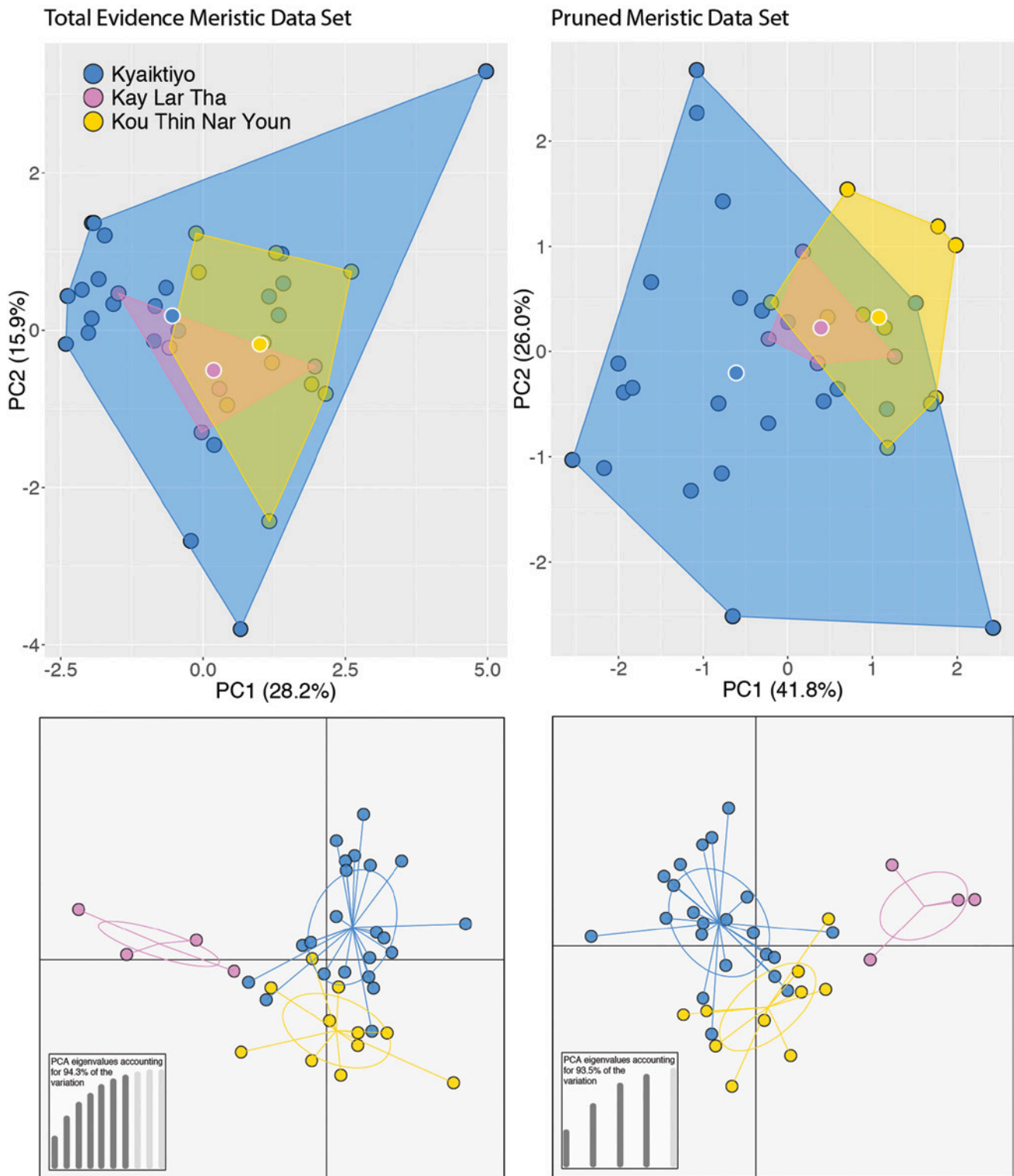


Figure 4. PCA and DAPC plots of the total evidence and pruned meristic data sets from the geographic variation analysis.

while de-emphasizing those characters that do not, thus increasing the overall accuracy of the model by eliminating noise and the potential of overfitting (Agarwal et al., 2007). This is especially true if there are 10 or more dimensions (i.e., characters).

Total evidence and pruned data sets

We ran separate PCAs and discriminant analyses of principal components (DAPC; see below for details) on total

evidence and pruned data sets generated from both the mensural and meristic data in both the integrative and geographic variation frameworks (i.e., a total of eight different analyses). In the first set of analyses, we maximized the dimensionality of the data sets by using all the characters analyzed (the total evidence data set). In the second set of analyses, we reduced the dimensionality of the total evidence data sets, by using only characters that had significantly different mean values between at least one pair

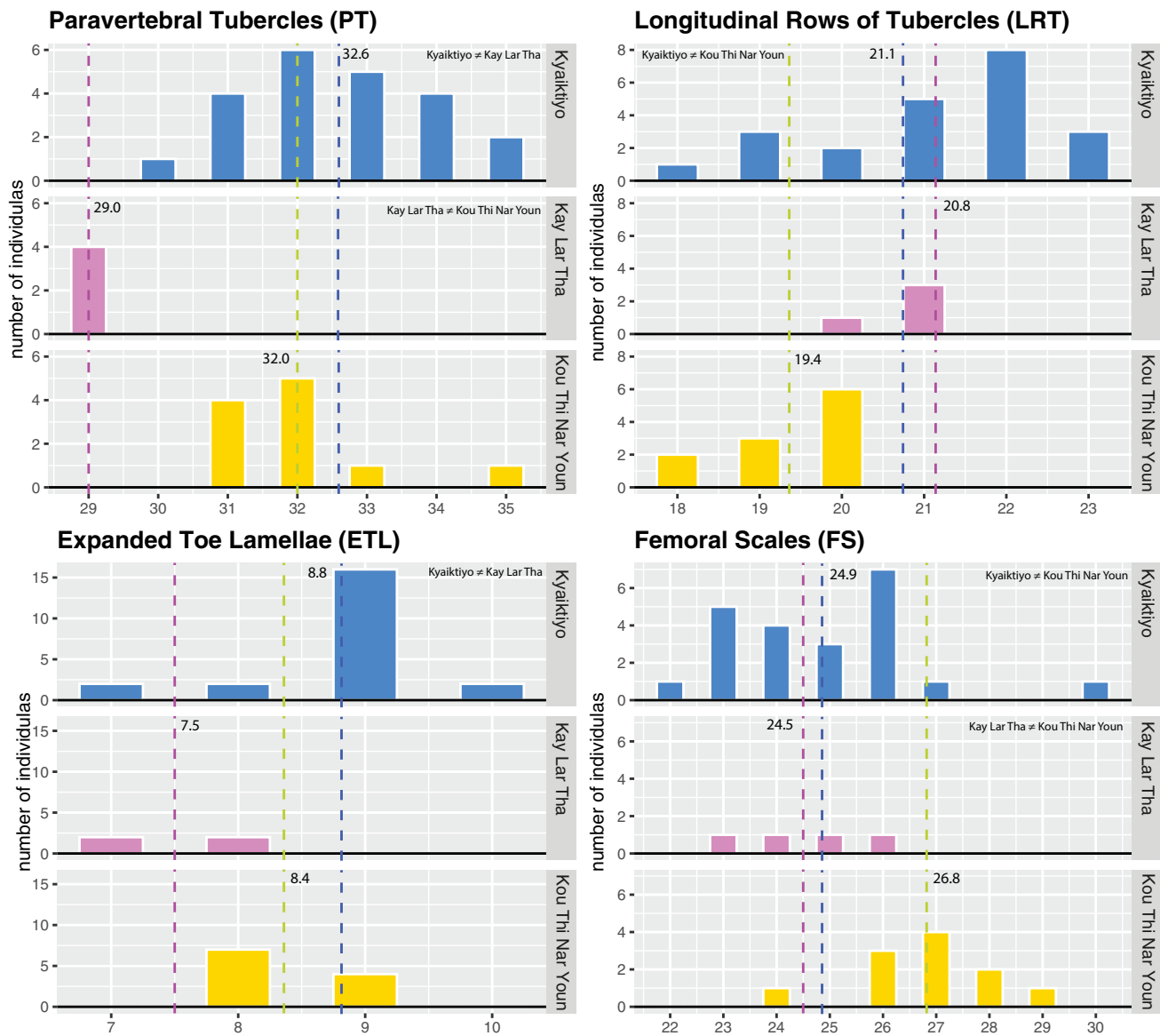


Figure 5. Histograms of the discrete meristic characters from the geographic variation analysis that differ significantly (\neq) in mean values between the species pairs listed on the plots. Mean values are plotted next to their respective vertical dashed lines.

of species as determined by the ANOVA and subsequent TukeyHSD tests (i.e., the pruned data sets). Mensural characters were scaled to SVL in order to completely remove any potential effects of allometry using the following equation: $X_{adj} = X - \beta(SVL - SVL_{mean})$, where X_{adj} = adjusted value; X = measured value; β = unstandardized regression coefficient for each OTU; and SVL_{mean} = overall average SVL of all OTU's (Thorpe, 1975, 1983; Turan, 1999; Leonart et al., 2000). Simply dividing each metric by SVL does not eliminate allometry.

PCA, implemented by the `prcomp()` command in R, is an indiscriminate analysis plotting the overall variation among individuals (i.e., the data points in the plot) while treating each individual independently (i.e., not coercing data points into pre-defined groups). Because the data in all data sets were potentially skewed by large ranges among the characters, all characters were log transformed and scaled to their standard deviation prior to analysis in order to normalize their distribution so as to ensure characters with very large and very low values did not over-leverage

the results owing to intervariable nonlinearity and to ensure the data were analyzed on the basis of correlation not covariance. In order to determine the number of interpretable PCs (i.e., those that capture the most amount of variation in the data set with the least amount of noise) to retain for downstream analyses prior to PC degeneration (i.e., subsequent PCs represent negligible structure in the data), a modified version of the broken stick model (Cangelosi and Gorieli, 2007) which uses a stopping rule (Jackson, 1993), was implemented with the VEGAN package in R (Oksanen et al., 2018) using the `bs()` command. This analysis produces overlapping curves of eigenvalues and broken stick values and proposes that the number of retained PCs should have eigenvalues higher than their corresponding random broken stick components. Retaining too many variables, forces false structure to appear in the data and retaining too few, runs the risk of missing true structure (Cangelosi and Gorieli, 2007). Factor loadings from the retained PCs for each population were then subjected to ANOVA and TukeyHSD tests in order to determine which

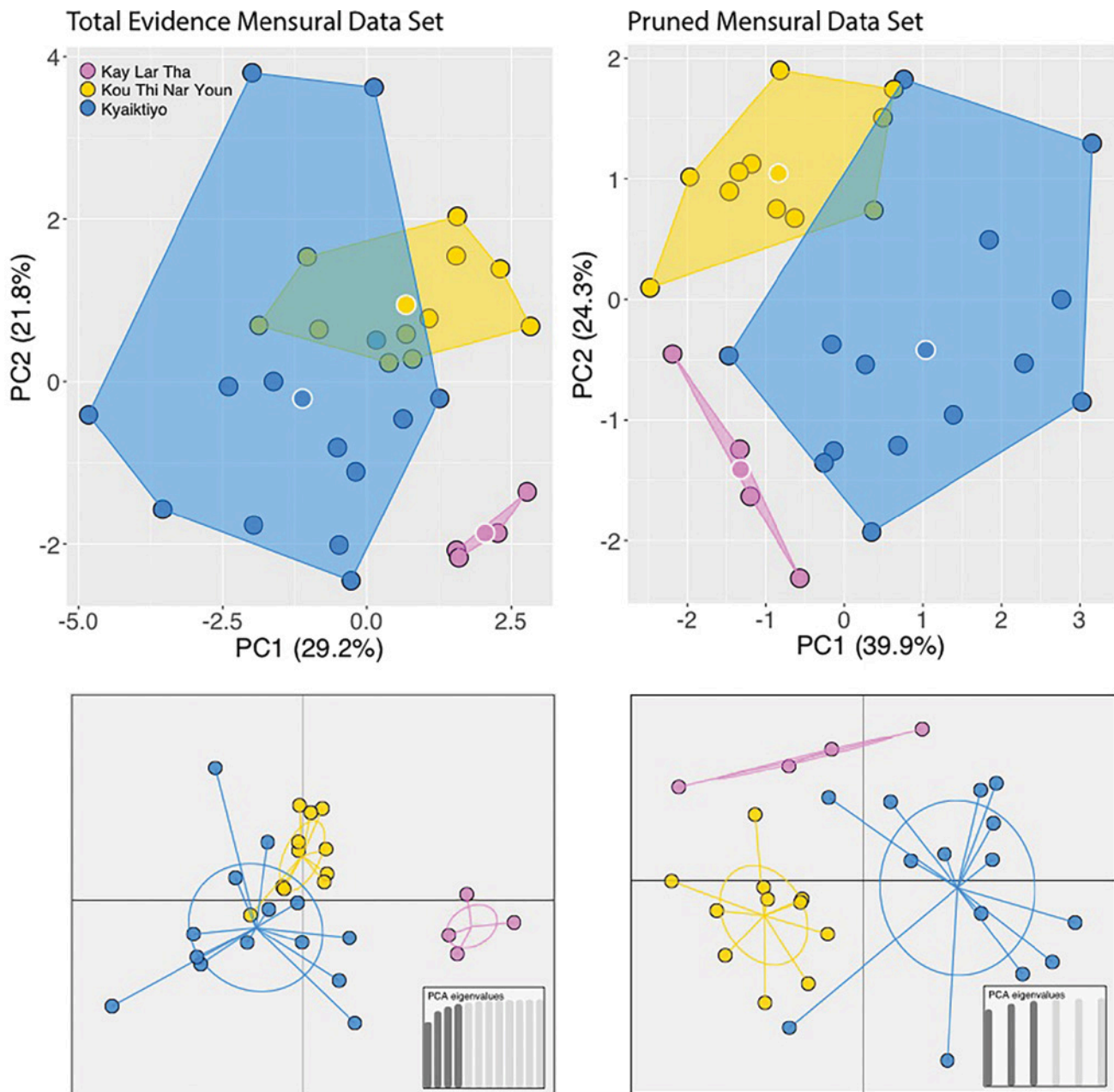


Figure 6. PCA and DAPC plots of the total evidence and pruned mensural data sets from the geographic variation analysis.

factor loading means (i.e., the approximation of centroid values) between which species pairs differed significantly ($p \leq 0.05$). This method evaluates whether or not each population occupies a statistically different position along the retained PCs from other populations, thus adding a more quantifiable interpretation of the PCA.

Based on factor loadings from a PCA generated as part of the `dapc()` command in R, a DAPC was performed on both the integrative and geographic variation data sets. The DAPC places the individuals of each predefined population into separate clusters (i.e., plots of points) bearing the smallest within-group variance that produce linear combinations of centroids having the greatest between-group variance (i.e., linear distance; Jombart et al., 2010). DAPC relies on scaled data from its own internally generated PCA as a prior step to ensure that variables analyzed are not correlated and number fewer than the sample size. Dimension

reduction of the DAPC prior to plotting, is accomplished by retaining the first set of PCs that account for approximately 90% of the variation in the data set (Jombart and Collins, 2015) as determined from a scree plot.

The raw morphological data for all analyses from the three populations are presented in Tables A1, A2, and A3 and their summary statistics in Table A4 in the Appendix. Uncorrected pairwise sequence divergences are in Table A5.

Results

Integrative analyses (two OTUs)

The ML and BI analyses recovered trees with identical topologies wherein *Cyrtodactylus aequalis* is weakly supported as monophyletic (BI 0.91/UFB 71) and most closely

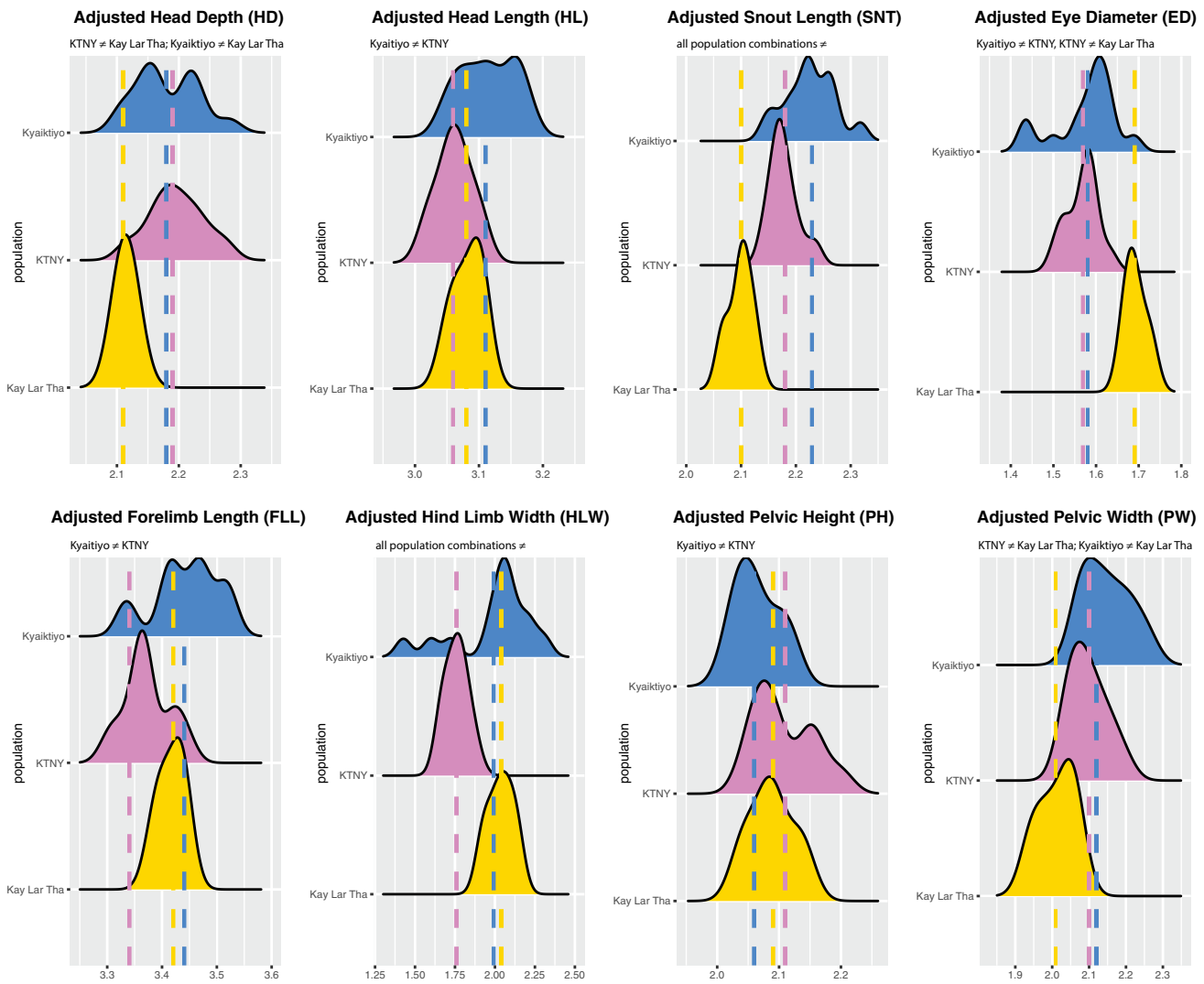


Figure 7. Ridge plots of the continuous mensural characters from the geographic variation analysis that differ significantly (\neq) in adjusted mean values between the species pairs listed above the plots. Mean values are represented by the vertical dashed lines.

related (1.00/100) to the sister species *C. bayinnyiensis* and *C. dattkyaikensis* from the Salween Basin of southeastern Myanmar (Fig. 1). The analyses recovered two strongly supported (1.00/100) reciprocally monophyletic lineages within *C. aequalis*—the Kay Lar Tha population and the combined Kyaiktiyo and Kou Thi Nar Youn populations. The latter forms a tricotomy composed of two lineages of individuals from Kyaiktiyo and another lineage from Kou Thi Nar Youn. However, branch lengths among individuals of the three populations are extremely short (nearly indiscernible in Fig. 1) with uncorrected pairwise sequence divergences ranging from 0.000–0.0014% (Table A5). As such, we consider the polytomous relationship among Kyaiktiyo and Kou Thi Nar Youn and their low genetic divergences (0.0001–0.0008%) as evidence that they should be considered a single population (KKTNY). Such a pattern aligns well with the topography surrounding their distribution, as gene flow is likely continuous through an arcuate range of low hills and mountains that connect their localities (Fig. 1). Thus, subsequent morphological analyses of *C. aequalis* within the integrative framework are

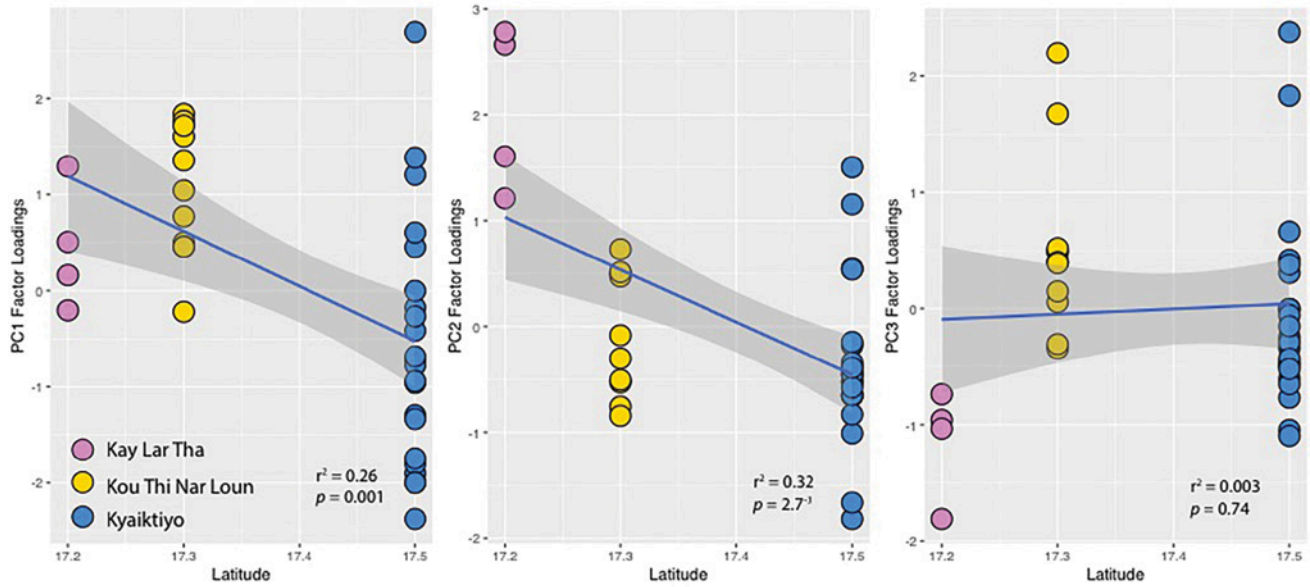
based only on the Kay Lar Tha and KKTNY lineages (i.e., two OTUs).

The BEAST analysis recovered the same topology as the ML and BI trees and the subsequent GMYC species delimitation analysis recovered the same eight ingroup species of the *Cyrotactylus sinyineensis* group delimited by Grismer et al. (2020) and the analyses herein (Fig. 1) with a highly significant likelihood ratio of 20.64461 ($p = 3.289127 \times 10^{-5}$). The GMYC recovered *C. aequalis* as a single species and did not separate out any of its sublineages of individuals as significantly different genetic clusters beyond the null.

Meristic data

In the total evidence meristic data set, the PCA showed that the Kay Lar Tha population was completely eclipsed by the KKTNY population along the combined ordination of the first two PCs which accounted for 44.2% of the variation (Fig. 2). PC1 loaded most heavily for IL, LT, VS, and FS, whereas PC2 loaded most heavily for ETL (Table 3). Based on an ANOVA and the subsequent TukeyHSD tests

Principal Component Factor Loadings from the Pruned Meristic Data Set



Principal Component Factor Loadings from the Pruned Mensural Data Set

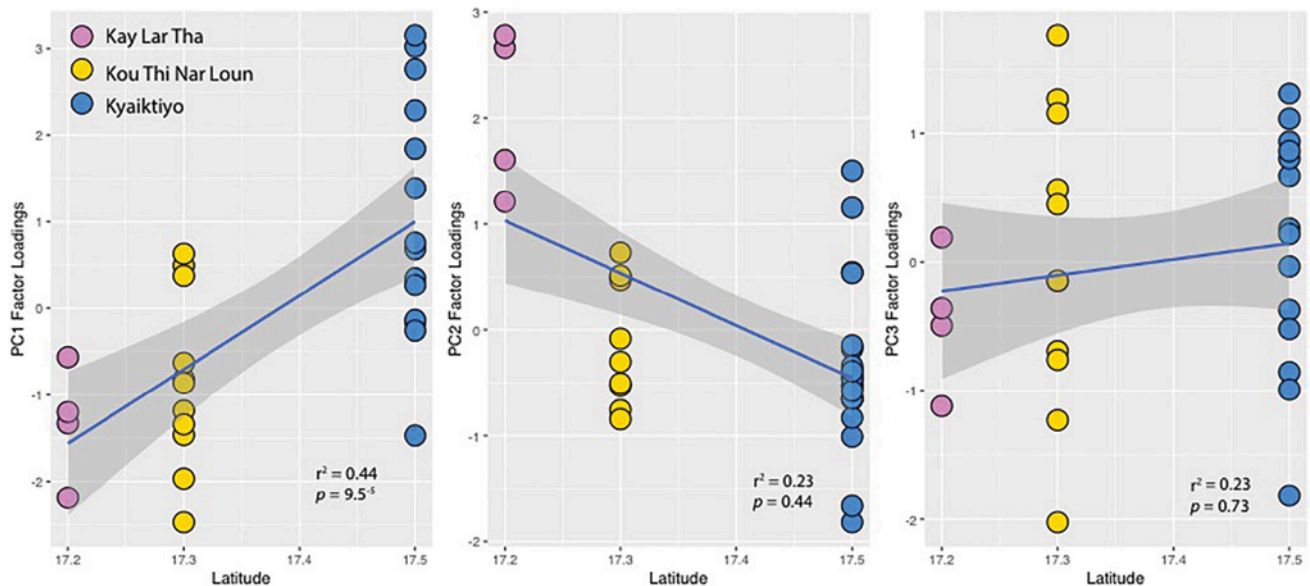


Figure 8. Factor loadings of PC1–PC3 from the pruned geographic variation analyses regressed against latitude.

(Table 4), a pruned data was constructed using only PV and TLE. In the PCA of the pruned data set, the KKTNY and Kay Lar Tha populations plotted separately along the PC1 but the former eclipsed the latter along PC2 (Fig. 2). Both characters loaded nearly equally along both PCs which accounted for 100.0% of the variation in the data set. The density plots of the first discriminant functions in the DAPC for both the total evidence and pruned analyses mirrored their respective PCAs (Fig. 2).

Mensural data

In the total evidence mensural data set, the PCA showed that the Kay Lar Tha population was completely eclipsed by the KKTNY population along the first two PCs which accounted for 73.8% of the variation (Fig. 3). PC1 loaded most heavily for SNT, ED, HDW, HLL, FLW, and FLL

whereas PC2 loaded most heavily for HL and HW (Table 5). Based on an ANOVA and subsequent TukeyHSD tests (Table 4), a pruned data set was constructed using only PW and HD. In the PCA of that data set, the KKTNY and Kay Lar Tha populations plotted separately along the PC1 but the former eclipsed the latter along PC2. Both characters loaded equally along both PCs. The density plots of the first discriminant functions in the DAPC for both analyses mirrored their respective PCAs (Fig. 3).

Comparison of PCA centroids

Broken stick models for all four data sets indicated that the most significant amount of variation occurred along the first two components. ANOVAs of the combined factor loadings of PC1 and PC2 for all four data sets recovered no significant differences between any species pairs, meaning

Table 3. Summary statistics and principal component analysis scores for the total evidence meristic integrative analysis data set of *Cyrtodactylus aequalis*. Abbreviations are listed in the Materials and methods.

	PC1	PC2	PC3	PC4	PC5	PC6	PC7	PC8	PC9	PC10
Standard deviation	1.681377815	1.260629875	1.23611354	1.123481024	0.983850292	0.829634646	0.695999807	0.632865868	0.501294877	0.033288645
Proportion of Variance	0.2827	0.15892	0.1528	0.12622	0.0968	0.06883	0.04844	0.04005	0.02513	0.00011
Cumulative Proportion	0.2827	0.44162	0.59442	0.72064	0.81744	0.88627	0.93471	0.97476	0.99989	1
Eigenvalue	2.82703	1.58919	1.52798	1.26221	0.96796	0.68829	0.48442	0.40052	0.2513	0.00111
SU	0.08471	0.19285	-0.21589	-0.74236	0.2709	-0.0701	0.19747	0.00837	0.49047	-0.00076
IL	0.40465	-0.10109	0.18371	-0.41994	0.31194	0.20407	-0.12682	0.04039	-0.67763	0.00913
PT	-0.16764	-0.29187	-0.45778	0.12911	0.42721	0.45449	-0.49398	0.00236	0.16547	0.00254
LT	-0.43686	-0.10023	-0.26981	-0.23058	-0.13123	-0.06912	0.10883	-0.73176	-0.32165	-0.01925
VS	0.42335	0.28572	0.04189	0.05961	-0.03831	-0.33528	-0.62703	-0.44972	0.15658	0.00305
TLE	-0.05969	0.61766	-0.31635	0.2477	0.34858	-0.08996	0.1422	0.08435	-0.2617	-0.47758
TLU	0.36648	-0.46174	-0.32989	-0.04979	-0.31664	-0.12758	0.05676	0.06312	0.0294	-0.64543
TTL	0.33865	-0.00868	-0.61731	0.15024	-0.06677	-0.20636	0.19949	0.10086	-0.17313	0.59549
FS	0.41405	0.12947	0.06204	0.21552	-0.02866	0.62181	0.38943	-0.43294	0.18638	-0.01431
PS	0.08315	-0.40519	0.20419	0.25749	0.63329	-0.41962	0.28462	-0.22774	0.10411	-0.00739

there were no significant differences among the positions of their centroids, indicating these two populations (KKT-NY & Kay Lar Tha) do not differ significantly from one another in multivariate space.

Geographic variation (three OTUs)

Meristic data

The PCA of the total evidence meristic data set using the three allopatric populations demonstrated that all three populations show considerable overlap along the first two PCs with closely spaced centroids (Fig. 4). The first two PCs accounted for 44.2% of the total variation with PC1 loading most heavily for IL, LT, VS, and FS and PC2 loading most heavily for ETL (Table 6). Based on an ANOVA and subsequent TukeyHSD tests (Table 4), a pruned data set based on four characters (PT, ETL, LT, FS; Fig. 5) demonstrated slightly less overlap between the Kyaiктиyo and Kou Thi Nar Youn populations along the first two PCs which accounted for 67.8% of the total variation (Fig. 4). PC1 loaded most heavily for LT and FS whereas PC2 loaded most heavily for ETL (Table 7). Broken stick models for both data sets indicated that the most significant amount of variation occurred along the first two components. An ANOVA of the summed factor loadings of PC1 and PC2 in the total evidence meristic data set indicated there were no significant differences between any species pairs, meaning there were no significant differences among the positions of the centroids and that these populations did not differ significantly from one another in morphospace. In the pruned data set, a significant difference (TukeysHSD $p = 0.0007$) in centroid placement was recovered between the Kyaiктиyo and the Kou Thi Nar Youn populations. The DAPC analyses for each data set showed no overlap in the 95% confidence ellipsoids among any populations (Fig. 4).

Mensural data

The PCA of the three populations using the total evidence mensural data set demonstrated reasonable separation among all three populations along the ordination of the first two PCs with widely spaced centroids (Fig. 6). The first two PCs account for 51.1% of the total variation with PC1 loading most heavily for HL, HW, and SNT and PC2 loading most heavily for HLW (Table 8). Based on an ANOVA and subsequent TukeyHSD tests (Table 4), a pruned data composed of eight characters (PH, PW, HL, HD, SNT, ED, HLW, and FLL; Fig. 7) demonstrated less overlap in the clusters of the Kyaiктиyo and Kou Thi Nar Youn populations with the first two PCs accounting for 64.2% of the total variation (Fig. 6). PC1 loaded most heavily for HL, SNT, and FLL and PC2 loaded most heavily for HLW (Table 9).

Broken stick models for both data sets indicated the most significant amount of variation occurred along the first three components. An ANOVA of the summed factor loadings of PC1–PC3 in the total evidence data set recovered no significant differences between any species pairs, indicating there were no significant differences in the centroid positions even though the Kay Lar Tha population clusters separately from the other populations along the

Table 4. Characters recovered by ANOVAs that bear significantly different mean values between population pairs in the meristic and mensural data sets and their subsequent TukeysHSD p values.

Geographic Variation Analyses		
Kyaiktiyo vs. Kou Thi Nar Youn	Kyaiktiyo vs. Kay Lar Tha	Kou Thi Nar Youn vs Kay Lar Tha
LT ($p = 0.001$)	PT ($p = 2.21E-05$)	PT ($p = 0.001$)
FS ($p = 0.008$)	ETL ($p = 0.002$)	FS ($p = 0.05$)
SNT ($p = 0.009$)	SNT ($p = 6.66E-06$)	SNT ($p = 0.003$)
HL ($p = 0.003$)	ED ($p = 0.004$)	ED ($p = 0.003$)
PH ($p = 0.039$)	HD ($p = 0.041$)	HD ($p = 0.014$)
HLW ($p = 0.01$)	PW ($p = 0.089$)	PW ($p = 0.05$)
FLL ($p = 0.023$)	Centroids (PC1–PC3, $p = 0.003$; pruned mensural data set)	HLW ($p = 0.038$)
Centroids (PC1 & PC2, $p = 0.0007$; pruned meristic data set)		
Centroids (PC1–PC3, $p = 0.003$; pruned mensural data set)		
Integrative Taxonomic Analyses		
Kyaiktiyo vs. KKTNY		
PT ($p = 1.29-05$)		
ETL ($p = 0.003$)		
HD ($p = 0.003$)		
PW ($p = 0.0003$)		

combined ordination of the first two components. However, the ANOVA and subsequent TukeyHSD tests (Table 4) of the pruned data set, recovered the centroid positions between the Kyaiktiyo and Kou Thi Nar Youn populations and the Kyaiktiyo and Kay Lar Tha populations as significantly different ($p = 0.003$ for both), indicating these population pairs differ significantly from one another in their positions in morphospace. The DAPC analyses for each data set recovered no overlap of the 95% confidence ellipsoids among any populations except for slight overlap between Kyaiktiyo and Kou Thi Nar Youn in total evidence data set (Fig. 6).

Morphospacial variation in relation to latitude

Factor loadings of the first three PCs in both the pruned meristic and pruned mensural data sets (i.e. the data sets with maximal variance) were regressed against the latitude (in decimal degrees) of each population in order to ascertain if there was evidence that overall variation in morphospace had a geographically clinal component. The factor loadings of PC1 and PC2 of the meristic data and PC1 of the mensural data showed a highly significant statistical clinal correlation with latitude ($p = 0.001$, 2.7^{-03} , and 9.5^{-05} , respectively) despite the fact latitude explained only 26%, 32% and 44%, respectively of the variation (Fig. 8). Factor loadings of PC3 of the meristic and PC2 and PC3 of the mensural data showed no significant correlation with latitude ($p = 0.74$, 0.44 , and 0.73 , respectively) although the slope of PC2 is suggestive of such.

Snout-vent length

Using the pruned mensural data set from the geographic variation analysis, we noted that individuals from the Kay Lar Tha population were shaped differently from similarly sized individuals between 64.0 mm and 79.0 mm SVL from the other two populations (Fig. 6). This may be due to

an inferred smaller adult SVL in the Kay Lar Tha population based on the smaller size of gravid females (64.9 mm vs. 78.5–87.1 mm; Fig. 9). However, we had only a single gravid individual from each population.

Color pattern

Although *Cyrtodactylus aequalis* can be diagnosed from other members of the *C. sinyineensis* group based on aspects of coloration and pattern (Grismer et al., 2018a, 2019c), color pattern among the individuals from the three localities is highly variable (Figs. 10, 11) and no consistent interpopulational diagnostic characteristics were recovered.

Discussion

This exercise highlights the necessity for an integrative approach to taxonomy. A prudent evaluation of the molecular evidence indicates that only one species should be recognized. Yet in the absence of these data, the combined statistical evidence from the meristic and mensural data sets (Table 4) coupled with the seemingly allopatric distribution among the three populations (Fig. 1) could underpin a compelling argument for the specific identity of all three populations. For example, in the geographic variation analyses the Kyaiktiyo and Kou Thi Nar Youn populations are shown to have significantly different mean values of LT, FS, SNT, HL, PH, HLW, FLL, and centroid positions in the pruned data sets (Table 4, Figs. 2, 3, 4, 5, 6–7). Yet the phylogeny indicates that the Kou Thi Nar Youn and Kyaiktiyo populations form a tricotomy with extremely low genetic divergence among the individuals of each lineage (0.000–0.0014%; Table A5). This suggests that gene flow currently exists among them, thus precluding their separate species independence despite the fact that each population comes from a different mountainous area (Fig. 1). However, some

Table 5. Summary statistics and principal component analysis scores for the total evidence mensural integrative analysis data set of *Cyrtodactylus aequalis*. Abbreviations are listed in the Materials and methods.

	PC1	PC2	PC3	PC4	PC5	PC6	PC7	PC8	PC9	PC10	PC11	PC12
Standard deviation	2.670531754	1.315235005	1.056338293	0.760788396	0.711881005	0.66099127	0.543839613	0.306000806	0.269940356	0.14498152	0.112385456	0.064556068
Proportion of Variance	0.59431	0.14415	0.09299	0.04823	0.04223	0.03641	0.02465	0.0078	0.00607	0.00175	0.00105	0.00035
Cumulative Proportion	0.59431	0.73847	0.83145	0.87969	0.92192	0.95833	0.98297	0.99078	0.99685	0.9986	0.99965	1
Eigenvalue	7.13174	1.72984	1.11585	0.5788	0.50677	0.43691	0.29576	0.09364	0.07287	0.02102	0.01263	0.00417
PW	-0.18227	0.3968	-0.31521	-0.69494	0.40644	-0.15127	-0.13354	0.05451	0.1136	0.06445	0.03301	0.00192
PH	0.0528	0.24889	0.84138	-0.07796	0.2451	0.13675	-0.37075	-0.00501	-0.05226	0.01757	-0.04428	-0.00251
AXG	-0.22776	-0.396	-0.05632	-0.32752	-0.0262	0.81574	-0.07218	0.05913	-0.03581	-0.06767	-0.00306	-0.01312
HL	-0.1802	0.4465	-0.35525	0.5329	0.06431	0.32073	-0.48859	-0.04292	0.08307	0.00016	-0.04741	-0.03548
HW	-0.21791	0.49507	0.14802	0.104	0.06813	0.295	0.74818	-0.02849	0.06424	-0.12312	0.05361	0.01666
HD	-0.23996	0.30898	0.08981	-0.26112	-0.84879	-0.07277	-0.15659	0.08312	-0.05996	-0.08174	0.03638	-0.04394
SNT	0.34933	0.19258	-0.0992	-0.0389	-0.06077	0.1917	0.09054	0.18756	-0.53102	0.6696	0.05754	-0.10977
ED	-0.3499	-0.13077	0.11371	0.15069	0.03622	-0.09949	0.03363	0.74681	0.36377	0.34331	-0.01935	-0.06484
HLW	-0.35914	-0.07569	0.00354	0.1167	0.17902	-0.15309	-0.05687	0.2007	-0.58903	-0.297	0.56034	-0.05926
HLL	0.36664	0.08791	-0.06714	-0.04051	0.03477	0.04821	0.01728	0.37512	-0.03343	-0.4629	-0.22553	-0.664
FLW	-0.36736	-0.04185	-0.0095	0.02848	0.07796	-0.13014	0.05047	0.01696	-0.44993	-0.0343	-0.78785	0.11052
FLL	0.36297	0.12026	-0.07738	-0.02085	-0.02198	0.09194	-0.0327	0.458	-0.06034	-0.31501	-0.03539	0.72352

Table 6. Summary statistics and principal component analysis scores for the total evidence meristic geographic variation data set of *Cyrtodactylus aequalis*. Abbreviations are listed in the Materials and methods.

	PC1	PC2	PC3	PC4	PC5	PC6	PC7	PC8	PC9	PC10
Standard Deviation	1.681377815	1.260629875	1.23611354	1.123481024	0.983850292	0.829634646	0.695999807	0.632865868	0.501294877	0.033288645
Proportion of Variance	0.2827	0.15892	0.1528	0.12622	0.0968	0.06883	0.04844	0.04005	0.02513	0.00011
Cumulative Proportion	0.2827	0.44162	0.59442	0.72064	0.81744	0.88627	0.93471	0.97476	0.99989	1
Eigenvalue	2.82703	1.58919	1.52798	1.26221	0.96796	0.68829	0.48442	0.40052	0.2513	0.00111
SU	0.08471	0.19285	-0.21589	-0.74236	0.2709	-0.0701	0.19747	0.00837	0.49047	-0.00076
IL	0.40465	-0.10109	0.18371	-0.41994	0.3194	0.20407	-0.12682	0.04039	-0.67763	0.00913
PT	-0.16764	-0.29187	-0.45778	0.12911	0.42721	0.45449	-0.49398	0.00236	0.16547	0.00254
LT	-0.43686	-0.10023	-0.26981	-0.23058	-0.13123	-0.06912	0.10883	-0.73176	-0.32165	-0.01925
VS	0.42335	0.28572	0.04189	0.05961	-0.03831	-0.33528	-0.62703	-0.44972	0.15658	0.00305
TLE	-0.05969	0.61766	-0.31635	0.2477	0.34858	-0.08996	0.1422	0.08435	-0.2617	-0.47758
TLU	0.36648	-0.46174	-0.32989	-0.04979	-0.31664	-0.12758	0.05676	0.06312	0.0294	-0.64543
TTL	0.33865	-0.00868	-0.61731	0.15024	-0.06677	-0.20636	0.19949	0.10086	-0.17313	0.59549
FS	0.41405	0.12947	0.06204	0.21552	-0.02866	0.62181	0.38943	-0.43294	0.18638	-0.01431
PS	0.08315	-0.40519	0.20419	0.25749	0.63329	-0.41962	0.28462	-0.22774	0.10411	-0.00739

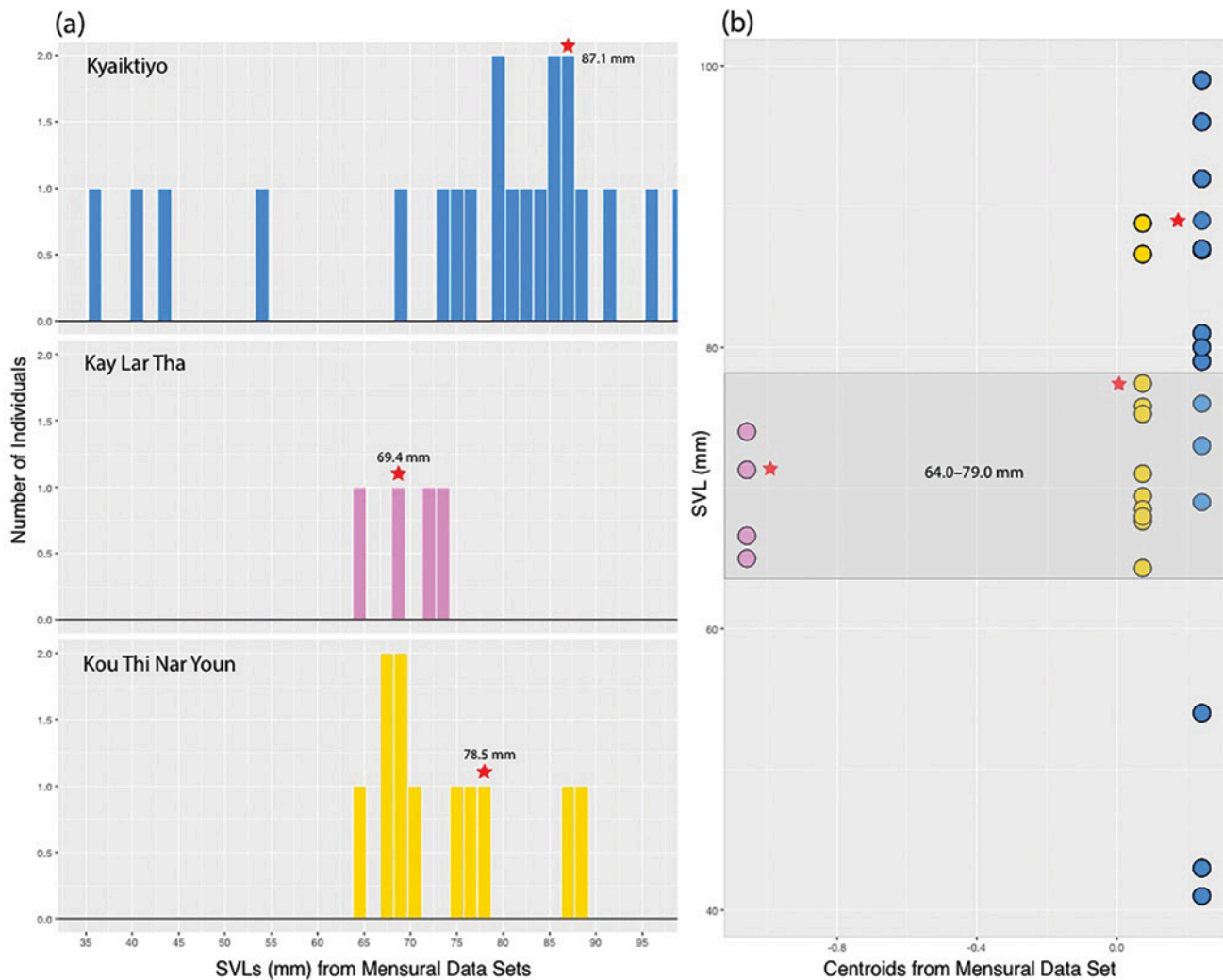


Figure 9. (a) Histograms illustrating the range of SVLs among the three populations. (b) SVLs regressed against body shape (centroid positions) represented by the mean values of the summed factor loadings of PC1–PC3 of the total evidence mensural data set. The centroid positions clearly separate the Kay Lar Tha populations from the others. Red stars indicate gravid females.

Table 7. Summary statistics and principal component analysis scores for the pruned meristic geographic variation data set of the populations of *Cyrtodactylus aequalis*. Abbreviations are listed in the Materials and methods.

	PC1	PC2	PC3	PC4
Standard deviation	1.292536637	1.020671118	0.904875374	0.684675155
Proportion of Variance	0.41766	0.26044	0.2047	0.1172
Cumulative Proportion eigen	0.41766	0.67811	0.8828	1
PV	1.670650959	1.041769532	0.818799442	0.468780068
LT	-0.437040744	-0.372721654	0.796499917	0.188843424
ETL	-0.657985268	0.057296631	-0.16031075	-0.733534558
FS	-0.003857408	-0.902089431	-0.430678829	0.027120575
	0.613217658	-0.209834038	0.392942861	-0.652326367

would consider their paraphyletic nature irrelevant and conclude that we are witnessing is speciation in the presence of gene flow (Hu et al., 2019). The Kyaiктиyo and Kay Lar Tha populations are allopatric, however, and differ significantly in mean values of PT, ETL, SNT, ED, HD, and PW (Table 4) yet differ only by a 0.001–0.004% sequence divergence. Furthermore, the Kay Lar Tha and the Kou Thi Nar Youn populations are allopatric and differ significantly in mean values of PT, FS, SNT, ED, HD, PW, and HLW (Table 4) but again differ only by a 0.011–0.015% sequence divergence (Table A5).

Much the same is true for the integrative analysis where the reciprocally monophyletic allopatric populations of KKTNY and Kay Lar Tha populations differ significantly in mean values of PT, ETL, HD, and PW (Table 4) but differ only by a 0.001–0.007% sequence divergence (Table A5). Weak genetic differentiation and pronounced morphological divergence could have resulted from historically high levels of gene flow and we are witnessing a population on the cusp of speciation.

The total evidence versus the pruned multivariate data sets in all analyses differed greatly in their percentage of PC

Table 8. Summary statistics and principal component analysis scores for the total evidence mensural geographic variation data set of *Cyrtodactylus aequalis*. Abbreviations are listed in the Materials and methods.

	PC1	PC2	PC3	PC4	PC5	PC6	PC7	PC8	PC9	PC10	PC11	PC12
Standard deviation	1.874706605	1.61882773	1.28840479	1.035328883	0.985286415	0.803995055	0.682321414	0.630322442	0.494470651	0.458761591	0.339868743	0.287121363
Proportion of Variance	0.29288	0.21838	0.13833	0.08933	0.0809	0.05387	0.0388	0.03311	0.02038	0.01754	0.00963	0.00687
Cumulative	0.29288	0.51126	0.64959	0.73892	0.81982	0.87368	0.91248	0.94559	0.96597	0.9835	0.99313	1
Proportion Eigenvalue	3.514524856	2.62060322	1.659986904	1.071905897	0.97078932	0.646408048	0.465562512	0.39730638	0.244501225	0.210462198	0.115510762	0.082438677
PW	-0.39222	-0.01638	0.02738	-0.4203	-0.10123	0.10608	-0.04298	0.78078	-0.14126	0.11136	-0.00908	-0.0556
PH	0.03647	0.0751	-0.66984	-0.08748	-0.19717	0.17416	0.56244	0.00137	0.20233	0.04749	-0.32636	-0.03791
AXG	0.22034	-0.02319	0.48273	-0.04039	-0.61997	-0.02683	0.09881	-0.01693	0.21696	0.44198	-0.24686	0.13324
HL	-0.40247	-0.03074	0.13164	0.3035	0.25987	0.4401	-0.19995	-0.00399	0.56605	0.10576	-0.29303	-0.09459
HW	-0.39271	0.06156	-0.31898	0.05399	-0.26325	0.14371	-0.34099	-0.36611	-0.3892	0.48798	0.085	0.01509
HD	-0.32996	0.27054	-0.19292	0.13439	-0.1974	-0.60402	-0.12678	0.08511	0.43452	-0.0893	0.18281	0.32453
SNT	-0.38295	0.24499	0.27664	-0.19741	-0.17313	-0.07508	0.31415	-0.30368	0.05497	-0.18484	0.18224	-0.61718
ED	0.08164	-0.42557	-0.16611	0.52134	-0.26808	-0.2349	-0.11541	0.26599	-0.03215	-0.01093	-0.00664	-0.5482
HLW	-0.12194	-0.51664	0.01136	-0.08644	0.29146	-0.12906	0.37933	-0.06464	0.18817	0.46497	0.45167	0.07303
HLL	-0.03916	-0.46987	-0.08931	-0.25404	-0.41507	0.3333	-0.20009	-0.15367	0.21665	-0.45911	0.27038	0.1653
FLW	-0.26238	-0.4224	0.03976	-0.28247	0.12215	-0.41693	-0.05999	-0.23409	-0.11852	-0.11589	-0.6284	0.04301
FL	-0.3642	-0.09157	0.21779	0.48826	-0.1293	0.12693	0.44743	0.05687	-0.36179	-0.24085	-0.02641	0.38378

factor loadings (6). The pruned data sets had higher loadings as a result of their reduced dimensionality resulting in significantly different centroid positions in three of the four data sets (Table 4) as compared to the total evidence data sets which had lower PC loadings and no significant differences in centroid positions. An argument could be marshaled that by pruning the variables based on information from the same data that is used in downstream analyses, we are forcing significantly different structure where it may not exist. Perhaps, but in practice all data sets are in effect pruned as dozens more meristic and mensural characters that could have been conceived were not evaluated. Had they been, it is highly likely would have obscured much of the signal in the data and reduced the accuracy of the analysis. Even in the total evidence data sets, we in effect pruned the data to focus only on characters that have been shown to be diagnostic for *Cyrtodactylus* (e.g., Grismer et al., 2012 and references therein)—some for well over a century (Gray, 1827).

In the total evidence data set, the PCAs for both the meristic and mensural data showed considerable overlap among all populations and there were no statistically different mean values among any pair of centroids. Yet the DAPCs for both analyses showed no overlap among the 95% confidence ellipsoids. So which set of analyses should underpin our taxonomic decisions? We argue that the uncoerced data set of a PCA bearing statistically different centroid placements is superior to a coerced DAPC where in effect, the taxonomy (i.e., groupings) is determined beforehand in the latter, often using the same data. The more agnostic approach of a PCA clusters individuals independently of one another.

PC loadings should also be taken into consideration when basing taxonomic decisions on a PCA. For example, an ANOVA of the summed factor loadings of PC1–PC3 in the total evidence meristic data set recovered no significant differences between any species pairs, indicating there were no significant differences in the centroid positions even though the Kay Lar Tha population does not overlap either of the other populations along the combined ordination of the first two components (Fig. 6). This is likely because the factor loadings accounted for only 29.2%, 21.8%, and 15.3% of the total variation, respectively, in the data set.

The Kay Lar Tha population

Under a strict adherence of the GLC as outlined herein, we might argue that speciation has already occurred and the Kay Lar Tha population should be described and named. It exists on the top of a mountain isolated in an agricultural flood plain, occurs only among boulders in a restrictive granite microhabitat, and bears several significantly different diagnostic characters from the KKTNY population, there is no evidence of current gene flow between them, and based on the size of gravid females, adults may be considerably smaller (Fig. 9). However, the GMYC analysis did not recover any of the sublineages of *C. aequalis* as separate, significantly different, genetic clusters beyond the null and evidence suggests the meristic and mensural variation have a strong geographic component (Fig. 8),

Table 9. Summary statistics and principal component analysis scores for the pruned mensural geographic variation data set of *Cyrtodactylus aequalis*. Abbreviations are listed in the Materials and methods.

	PC1	PC2	PC3	PC4	PC5	PC6
Standard deviation	1.547170035	1.208627314	0.966606177	0.693630816	0.632704035	0.574211888
Proportion of Variance	0.39896	0.24346	0.15572	0.08019	0.06672	0.05495
Cumulative Proportion	0.39896	0.64242	0.79814	0.87833	0.94505	1
Eigenvalue	2.393735116	1.460779985	0.934327501	0.48112371	0.400314396	0.329719293
PH	-0.20366	0.4134	-0.79371	0.18749	-0.27042	0.2222
HL	0.52039	-0.19982	-0.12543	0.54091	0.41853	0.45364
HD	0.37427	0.53759	-0.18133	-0.29793	0.54497	-0.39024
SNT	0.50911	0.25198	0.17963	-0.45513	-0.4226	0.50922
HLW	0.06532	-0.63368	-0.51267	-0.55763	0.13602	0.0436
FLL	0.53308	-0.18743	-0.16221	0.25577	-0.50756	-0.57563

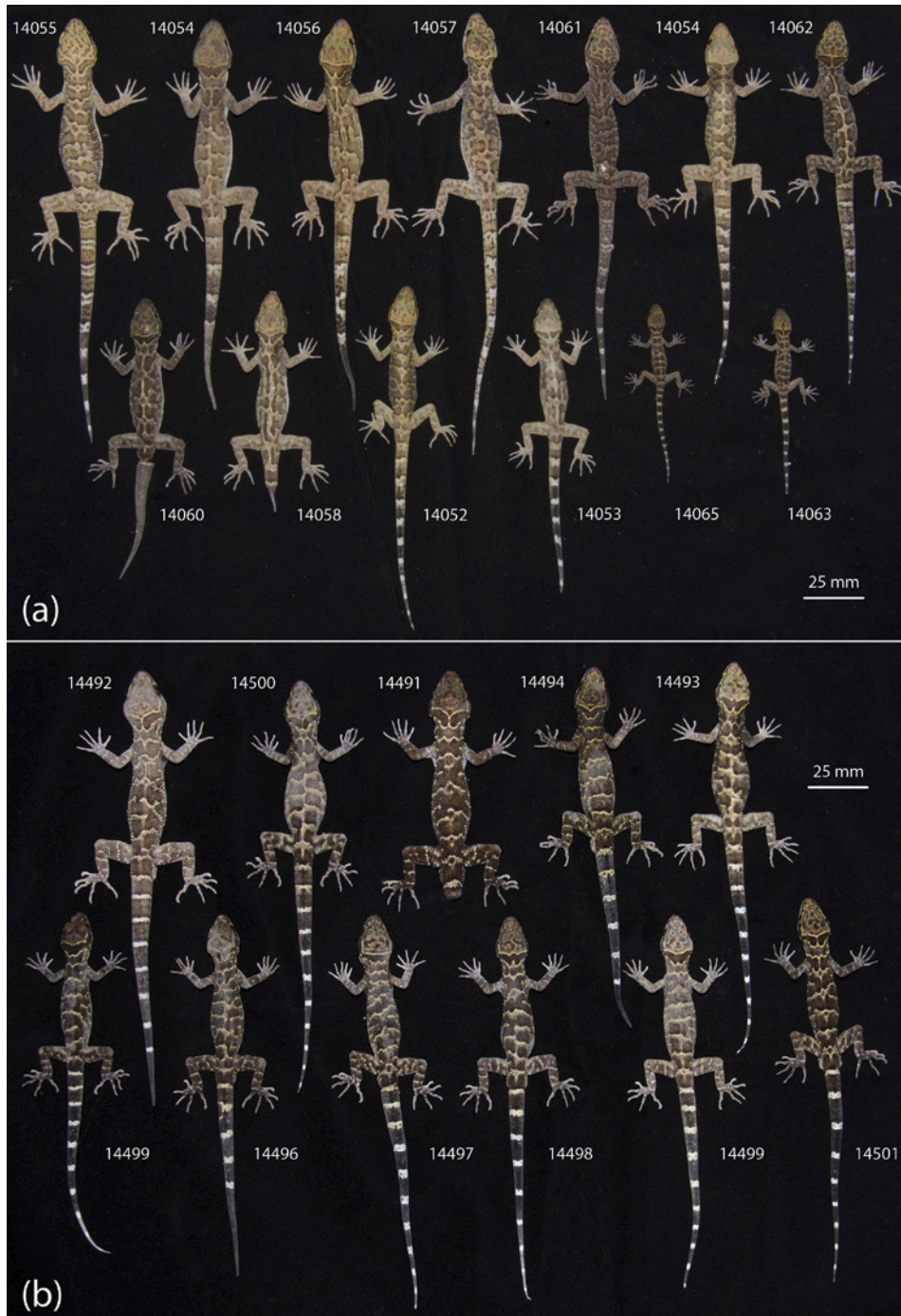


Figure 10. (a) Color pattern variation in a series of *Cyrtodactylus aequalis* from Kyaiktiyo Mountain, Mon State, Myanmar. (b) Color pattern variation in a series of *C. aequalis* from Kou Thi Nar Youn, Mon State, Myanmar. Numbers refer to the La Sierra University Herpetological Collection (LSUHC).

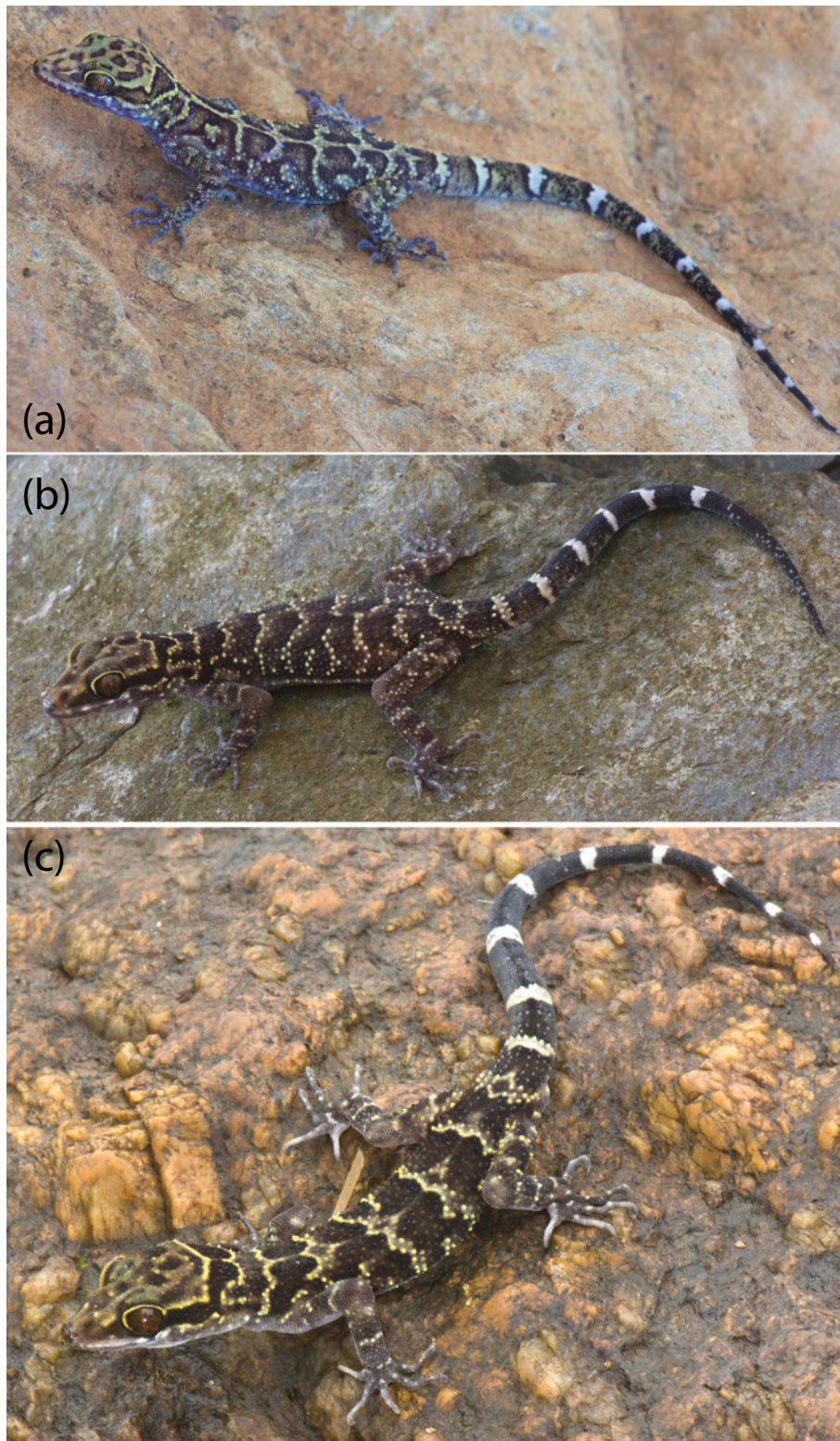


Figure 11. Comparison of living individuals of *Cyrtodactylus aequalis* from Mon State, Myanmar: (a) adult female LSUHC 14062 from Kyai-ktiyo Mountain, (b) adult female LSUHC 14496 from Kay Lar Tha, and (c) adult male LSUHC 14501 from Kou Thi Nar Youn.

suggesting current or at least very recent gene flow, or environmental factors influencing phenotype. As such we depart from a strict adherence to the GLC and elect consider this population as *C. aequalis*, thus removing its *con ferre* designation (sec., Grismer et al., 2020).

Conservation implications

Although we illustrate the significant role that integrative analyses should play in bringing our taxonomies in line with evolutionary history and avoiding over or underestimating biodiversity, this is not always possible. Many analyses are based on museum specimens collected long before tissue samples would have been taken and unfortunately and surprisingly, some taxonomists *still* do not take tissue samples from the specimens they collect. In such cases, prudent morphological analyses should be employed in order to form legitimate, testable species-designation hypotheses. Given the current biodiversity crisis—especially in the imperiled tropical regions of Indochina and Southeast Asia—this is often the only option taxonomist working with rare or poorly known species have in order to lobby for taxonomy-based implementation of legislative protection.

Acknowledgements

We wish to thank Mr. Win Naing Thaw of the Ministry of Natural Resources and Environmental Conservation Forest Department for the collection and export permits. LLG thanks the College of Arts and Sciences of La Sierra University and Fauna & Flora International for partial funding. JRO was supported by funding from the National Science Foundation of the USA (DEB 1656004). This paper is contribution number 889 of the Auburn University Museum of Natural History.

References

- Acinas, S.G., Klepac-Ceraj, V., Hunt, D.E., Pharino, C., Ceraj I., Distel, D.L., Polz, M.F. (2004) Fine-scale phylogenetic architecture of a complex bacterial community. *Nature* 430, pp. 551–554.
- Agarwal, A., El-Ghazawi, T., El-Askary, H., Le-Moigne, J. (2007) Efficient hierarchical-PCA dimension reduction for hyperspectral imagery. 2007 IEEE International Symposium on Signal Processing and Information Technology. DOI: 10.1109/ISSPIT.2007.4458191.
- Agarwal, I., Bauer, A.M., Jackman, T.R., Karanth, K.P. (2014) Insights into Himalayan biogeography from geckos: a molecular phylogeny of *Cyrtodactylus* (Squamata: Gekkonidae). *Mol. Phylogenet. Evol.* 80, pp. 145–155.
- Ahrens, D., Fabrizi, S., Šipek, P., Lago, P.K. (2013) Integrative analysis of DNA phylogeography and morphology of the European rose chafer (*Cetonia aurata*) to infer species taxonomy and patterns of postglacial colonisation in Europe. *Mol. Phylogenet. Evol.* 69, pp. 83–94.
- Barracough, T.G., Birky, C.W., Jr., Burt, A. (2003) Diversification in sexual and asexual organisms. *Evol.* 57, pp. 2166–2172.
- Bauer, A.M. (2003) Descriptions of seven new *Cyrtodactylus* (Squamata: Gekkonidae) with a key to the species of Myanmar (Burma). *Proc. Cal. Acad. Sci.* 54, pp. 463–498.
- Cangelosi, R., Goriely, A. (2007) Component retention in principal component analysis with application of cDNA microarray data. *Biology Direct*, 2, p. 2.
- Connette, G.M., Oswald, P., Thura, M.K., Connette, K.J.L., Grindley, M.E., Songer, M., Zug, G.R., Mulchay, D.G. (2017) Rapid forest clearing in a Myanmar proposed national park threatens two newly discovered species of geckos (Gekkonidae: *Cyrtodactylus*). *PLoS ONE* 12:e0174432.
- Coyne, J.A., Orr, H.A. (1998) The evolutionary genetics of speciation. *Phil. Trans. R. S. London B* 353, pp. 287–305.
- De Queiroz K. (2007) Species concepts and species delimitation. *Syst. Biol.* 56, pp. 879–886.
- Drummond, A.J., Suchard, M.A., Xie, D., Rambaut, A. (2012) Bayesian Phylogenetics with BEAUti and BEAST 1.7. *Mol. Biol. Evol.* 29, pp. 1969–1973.
- Fontaneto, D., Herniou, E.A., Boschetti, C., Caprioli, M., Melone, G., Ricci, C., Barrenclough, T.G. (2007) Independently evolving species in asexual bdelloid rotifers. *PLoS Biol.* 5, e87.
- Fujisawa, T., Barraclough, T.G. (2013) Delimiting species using single-locus data and the Generalized Mixed Yule Coalescent approach: a revised method and evaluation on simulated data sets. *Syst. Biol.* 62, pp. 707–724.
- Gray, J.E. (1827) A synopsis of the genera of saurian reptiles, in which some new genera are introduced, and the others reviewed by actual examination. *Philosophical Magazine*, 2, pp. 54–58.
- Grismer, L.L., Grismer, J.L. (2017) A re-evaluation of the phylogenetic relationships of the *Cyrtodactylus condorensis* group (Squamata; Gekkonidae) and a suggested protocol for the characterization of rock-dwelling ecomorphology in *Cyrtodactylus*. *Zootaxa* 4300, pp. 486–504.
- Grismer, L.L., Wood, Jr., P.L., Myint Kyaw Thura, Zin, T., Quah, E.S.H., Murdoch, M.L., Grismer, M.S., Lin, A., Kyaw, H., Ngwe L. (2018a) Twelve new species of *Cyrtodactylus* Gray (Squamata: Gekkonidae) from isolated limestone habitats in east-central and southern Myanmar demonstrate high localized diversity and unprecedented microendemism. *Zool. J. Linn. Soc.* 182, pp. 862–959.
- Grismer, L.L., Wood, Jr., P.L., Myint Kyaw Thura, Zin, T., Quah, E.S.H., Murdoch, M.L., Grismer, M.S., Herr, M.W., Lin A., Kyaw, H. (2018b) Three more new species of *Cyrtodactylus* (Squamata: Gekkonidae) from the Salween Basin of eastern Myanmar underscores the urgent need for the conservation of karst habitats. *J. Nat. Hist.* 52, pp. 1243–1294.
- Grismer, L.L., Wood, Jr., P.L., Myint Kyaw Thura, Quah, E.S.H., Grismer, M.S., Murdoch, M.L., Espinoza, R.E., Aung Lin. (2018c) A new *Cyrtodactylus* Gray (Squamata, Gekkonidae) from the Shan Hills and the biogeography of Bent-toed Geckos from eastern Myanmar. *Zootaxa*, 4446, pp. 477–500.
- Grismer, L.L., Wood, Jr., P.L., Quah, E.S.H., Myint Kyaw Thura, Murdoch, M.L., Grismer, M.S., Herr, M.W., Espinoza, R.E., Brown, R.M., Aung Lin. (2018d) Phylogenetic taxonomy of the *Cyrtodactylus peguensis* group (Reptilia: Squamata: Gekkonidae) with descriptions of two new species from Myanmar. *PeerJ*, 6:e5575.
- Grismer, L.L., Wood, Jr., P.L., Myint Kyaw Thura, Nay Myo Win, Grismer, M.S., Trueblood, L.A., Quah, E.H.S. (2018e) A re-description of *Cyrtodactylus chrysopylos* Bauer (Squamata: Gekkonidae) with comments on the adaptive significance of bright coloration in hatchlings and descriptions of two new species from eastern Myanmar (Burma). *Zootaxa*, 4527, pp. 151–185.
- Grismer, L.L., Wood, Jr., P.L., Myint Kyaw Thura, Nay Myo Win, Quah, E.S.H. (2018f) Two more new species of the *Cyrtodactylus peguensis* group (Squamata: Gekkonidae) from the fringes of the Ayeyarwady Basin, Myanmar. *Zootaxa* 4577, pp. 274–294.
- Grismer, L.L., Wood, Jr., P.L., Quah, E.S.H., Myint Kya Thura, Herr, M.X., Aing Ko Lin (2019a) A new species of forest-dwelling *Cyrtodactylus* (Squamata: Gekkonidae) from Indawgyi Wildlife Sanctuary, Kachin State, Myanmar. *Zootaxa* pp. 1–25.
- Grismer, L.L., Wood, Jr., P.L., Quah, E.S.H., Myint Kya Thura, Oaks, J.R., Aung Lin (2019b) A new species of Bent-toed Gecko (Squamata, Gekkonidae, *Cyrtodactylus*) from the

- Shan Plateau in eastern Myanmar (Burma). *Zootaxa* 4624, pp. 301–321.
- Grismer, L.L., Wood, Jr., P.L., Quah, E.S.H., Grismer, M.S., Thura, M.K., Oaks, J.R., Lin, A. (2020) Two new species of *Cyrtodactylus* Gray, 1827 (Squamata: Gekkonidae) from a karstic archipelago in the Salween Basin of southern Myanmar (Burma). *Zootaxa* 4718, pp. 151–183.
- Grismer, L.L., Wood, Jr., P.L., Quah, E.S.H., Anuar, S., Muin, M.A., Sumontha, M., Norhayati, A., Bauer, A.M., Wangkulangkul, S., Grismer, J.L., Pauwels, O.S.G. (2012) A phylogeny and taxonomy of the Thai-Malay Peninsula Bent-toed Geckos of the *Cyrtodactylus pulchellus* complex (Squamata: Gekkonidae): combined morphological and molecular analyses with descriptions of seven new species. *Zootaxa*, 3520, pp. 1–55.
- Hillis, D.M. (2019) Species delimitation in herpetology. *J. Herpetol.* 53, pp. 3–12.
- Hoang, D.T., Chernomor, O., von Haeseler, A., Minh, B.Q., Vinh, L.S. (2018) UFBBoot2: Improving the ultrafast bootstrap approximation. *Mol. Biol. Evol.* 35, pp. 518–522.
- Hu, C.C., Wu, Y.-Q., Ma, L., Chen, Y.-J., Ji, X. (2019) Genetic and morphological divergence among three closely related *Phrynocephalus* species (Agamidae). *BMC Evol. Biol.* 19:114, pp. 1–15.
- Huelsenbeck, J.P., Ronquist, F., Nielsen, R., Bollback, J.P. (2001) Bayesian Inference of Phylogeny and Its Impact on Evolutionary Biology. *Science* 294, pp. 2310–2314.
- Jackson, D.A. (1993) Stopping rules in principle component analysis: a comparison of heuristical and statistical approaches. *Ecol.* 74, 2204–2214.
- Jombart, T., Devillard, S., Balloux, F. (2010) Discriminant analysis of principal components: a new method for the analysis of genetically structured populations. *BMC Genetics*, 11, 94.
- Jombart, T., Collins, C. 2015. A tutorial for discriminant analysis of principal components (DAPC) using adegenet 2.0.0. Available at: <http://adegenet.r-forge.r-project.org/files/tutorial-dapc-pdf>.
- Kalyaanamoorthy, S., Minh, B.Q., Wong, T.K., von Haeseler, A., Jermini, L.S. (2017) ModelFinder: fast model selection for accurate phylogenetic estimates. *Nature Methods* 14, p. 587.
- Katoh, M., Kuma, M. (2002) MAFFT: a novel method for rapid sequence alignment based on fast Fourier transform. *Nuc. Acids Res.* 30, pp. 3059–3066.
- Knowles, L.L., Carstens, B.C. (2007) Delimiting species without monophyletic gene trees. *Syst. Biol.* 56, pp. 887–895.
- Kumar, S., Stecher, G., Tamura, K. (2016) MEGA7: Molecular evolutionary genetics analysis version 7.0 for bigger datasets. *Mol. Biol. Evol.* 33, pp. 1870–1874.
- Leaché, A.D., Koo, M.S., Spencer, C.L., Papenfuss, T.J., Fisher, R.N., McGuire, J.A. (2009) Quantifying ecological, morphological, and genetic variation to delimit species in the coast horned lizard species complex (*Phrynosoma*). *Proc. Nat. Acad. Sci.* 106, pp. 12418–12423.
- Lleonart, J., Salat, J., Torres, G.J. (2000) Removing allometric effects of body size in morphological analysis. *J. Theor. Biol.* 205, pp. 85–93.
- Macey, J.R., Larson, A., Ananjeva, N.B., Fang, Z., Papenfuss, T.J. (1997) Two novel gene orders and the role of light-strand replication in rearrangement of the vertebrate mitochondrial genome. *Mol. Biol. Evol.* 14, pp. 91–104.
- Maddison, W.P. & Maddison, D.R. (2015) *Mesquite: a modular system for evolutionary analysis*. Version 3.04. Available at: <http://mesquiteproject.org>.
- Mathews, L.M., Adams, L., Anderson, E., Basile, M., Gottardi, E., Buckholt, M.A. (2008) Genetic and morphological evidence for substantial hidden biodiversity in a freshwater crayfish species complex. *Mol. Phylogenet. Evol.* 48, pp. 126–35.
- Miller, M.A., Pfeiffer, W., Schwartz, T. (2010) Creating the CIPRES Science Gateway for inference of large phylogenetic trees. In: Proceedings of the Gateway Computing Environments Workshop (GCE), 14 Nov. 2010, New Orleans, LA pp. 1–8.
- Minh, Q., Nguyen, M.A.T., von Haeseler, A. (2013) Ultrafast approximation for phylogenetic bootstrap. *Mol. Biol. Evol.* 30, pp. 1188–1195.
- Oksanen, J.G., Blanchet, F.G., Friendly, M., Kindt, R., Legendre, P., McGlinn, D., Minchin, P.R., O'Hara, R.B., Simpson, G.L., Solymos, P., Henry, M., Stevens, H., Szoecs, E., Wagner, H. (2018). Community ecology package. <https://cran.r-project.org>.
- Nguyen, L.-T., Schmidt, H.A., von Haeseler, A., Minh, B.Q. (2015) IQ-TREE: A fast and effective stochastic algorithm for estimating maximum likelihood phylogenies. *Mol. Biol. Evol.* 32, pp. 268–274.
- Padial J.M., Miralles, A., de la Rivera, I., Vences, M. (2010) The integrative future of taxonomy. *Front. Zool.* 7, pp. 1–14.
- Pons, J., Barraclough, T.G., Gomez-Zurita, J., Cardoso, A., Duran, D.P., Hazell, S., Kamoun, S., Sumlin, W.D., Vogler, A.P. (2006) Sequence-based species delimitation for the DNA taxonomy of undescribed insects. *Syst. Biol.* 55, pp. 595–609.
- R Core Team. (2018) R: A language and environment for statistical computing. R Foundation for Statistical Computing. Vienna. [accessed 2018]. <http://www.R-project.org>.
- Rambaut A, Drummond, A.J. (2013) *TreeAnnotator v1.8.0 MCMC Output Analysis*. <http://dx.doi.org/10.1017/cbo9780511819049.020>.
- Rambaut A, Suchard, M.A., Xie, D., Drummond, A.J. (2014) *Tracer v1.6*. <http://dx.doi.org/10.1093/sysbio/syy032>.
- Ronquist, F., Teslenko, M., van der Mark, P., Ayres, D.L., Darling, A., Höhna, B., Larget, L., Liu, L., Suchard, M.A., Huelsenbeck, J.P. (2012) Mr. Bayes 3.2: efficient Bayesian phylogenetic inference and model choice across a large model space. *Syst. Biol.* 61, pp. 539–542.
- Satler, J.D., Carstens, B.C., Hedin, M. (2013) Multilocus species delimitation in a complex of morphologically conserved trapdoor spiders (Mygalomorphae, Antrodiaetidae, *Aliatyphus*). *Syst. Biol.* 62, pp. 805–23.
- Schild, D.R., Adams, R.H., Card, D.C., Corbin, A.B., Jezkova, T., Hales, N.R., Meik, J.M., Perry, B.W., Spencer, C.L., Smith, L.L., Garcia, G.C., Bouzid, N.M., Strickland, J.L., Parkinson, C.L., Borja, M., Castañeda-Gaytán, G., Bryson, R.W., Jr., Flores-Villela, O.A., Mackessy, S.P., Castoe, T.A. (2018) Cryptic genetic diversity, population structure, and gene flow in the Mojave rattlesnake (*Crotalus scutulatus*). *Mol. Phylogenet. Evol.* 127, 669–681.
- Sukumaran, J., Knowles, L.L. (2017) Multispecies coalescent delimits structure, not species. *Proc. Nat. Acad. Sci.* 114, pp. 1607–1612.
- Thorpe, R.S. (1975) Quantitative handling of characters useful in snake systematics with particular reference to interspecific variation in the Ringed Snake *Natrix natrix* (L.). *Biol. J. Linn. Soc.* 7, pp. 27–43.
- Thorpe, R.S. (1983) A review of the numerical methods for recognizing and analysing racial differentiation. In: J. Felsenstein, Editor *Numerical Taxonomy*. NATO ASI Series (Series G: Ecological Sciences), vol. 1. Springer-Verlag, Berlin, 404–423 pp.
- Trifinopoulos, J., Nguyen, L.-T., von Haeseler, A., Minh, B.Q. (2016) W-IQ-TREE: a fast online phylogenetic tool for maximum likelihood analysis. *Nuc. Acids Res.* 44, pp. W232–W235
- Turan, C. (1999) A note on the examination of morphometric differentiation among fish populations: The Truss System. *Turkish J. Zool.* 23, pp. 259–263.
- Watson, J.A., Spencer, C.L., Schild, D.R., Butler, B.O., Smith, L.L., Flores-Villela, O., Campbell, J.A., Mackessy, S.P., Castoe, T.A., Meik, J.M. (2019) Geographic variation in morphology in the Mohave Rattlesnake (*Crotalus scutulatus* (Kennicott 1861) (Serpentes: Viperidae): implications for species boundaries. *Zootaxa* 4683, pp. 129–143.
- Wilcox, T.P., Zwickl, D.J., Heath, T.A., Hillis, D.M. (2002) Phylogenetic relationships of the Dwarf Boas and a comparison of Bayesian and bootstrap measures of phylogenetic support. *Mol. Phylogenet. Evol.* 25, pp. 361–371.
- Wood, Jr., P.L., Heinicke, M.P., Jackman, T.R., Bauer, A.M. (2012) Phylogeny of bent-toed geckos (*Cyrtodactylus*) reveals a west to east pattern of diversification. *Mol. Phylogenet. Evol.* 65, pp. 992–1003.

Appendix

Table A1. Meristic and mensural data from the Kay Lar Tha population of *Cyrtodactylus aequalis*. R = right, L = left, / = data unobtainable or not applicable, r = regenerated.

Sex	LSUHC	LSUHC	LSUHC	LSUHC
	14242	14243	14244	14245
	f	f	f	f
Supralabials	8	8	8	8
Infralabials	6	7	7	7
Body tubercles low, weakly keeled	no	no	no	no
Body tubercles raised, moderately to strongly keeled	yes	yes	yes	yes
Paravertebral tubercles	29	29	29	29
Longitudinal rows of body tubercles	21	21	20	21
Tubercles extend beyond base of tail	yes	yes	yes	yes
Ventral scales	25	24	25	24
Expanded subdigital lamellae on 4th toe	7	7	8	8
Unmodified subdigital lamellae on 4th toe	16	15	16	13
Total subdigital lamellae on 4th toe	23	22	24	21
Enlarged femoral scales (R/L)	12/13	12/12	13/13	11/12
Total femoral scales	25	24	26	23
Femoral pores (R/L)	/	/	/	/
Total femoral pores in males	/	/	/	/
Enlarged Precolacal scales	8	9	9	9
Precolacal pores	/	/	/	/
Post-precolacal scales rows	3	3	3	3
Enlarged femoral and precolacal scales continuous	yes	yes	yes	yes
Pore-bearing femoral and precolacal scales continuous	/	/	/	/
Enlarged proximal femoral scales ~1/2 size of distal femorals	no	no	no	no
Medial subcaudals 2 or 3 times wider than long	yes	yes	yes	yes
Medial subcaudals extend onto lateral surface of tail	no	no	no	no
SVL	71.3	74.0	69.4	65.0
TL	85r	95.0	80.0	87.0
TW	6.9	7.2	6.0	5.4
FL	11.1	10.5	10.5	9.9
TBL	13.8	13.1	12.1	12.3
AG	33.0	30.1	25.1	27.6
HL	20.7	20.6	18.9	18.3
HW	14.0	13.7	12.8	12.6
HD	7.6	8.5	7.3	7.7
ED	4.9	5.0	4.7	4.4
EE	5.9	5.5	5.5	4.9
ES	8.4	7.1	7.4	7.5
EN	6.3	5.9	5.8	5.2
IO	5.1	5.4	4.3	4.5
EL	1.3	2.0	1.7	1.6
IN	2.4	2.1	2.2	2.0

Table A2. Meristic and mensural data from the Kyaiktiyo population of *Cyrtodactylus aequalis*. R = right, L = left, / = data unobtainable or not applicable, r = regenerated.

	29.5	25.0	31.8	39.8	35.1	35.68	33.51	40.6	30.11	36.12	33.83	18.72	15.58	16.42	33.08
AG	29.5	25.0	31.8	39.8	35.1	35.68	33.51	40.6	30.11	36.12	33.83	18.72	15.58	16.42	33.08
HL	21.4	19.9	22.3	26.2	26.1	24.79	23.31	26	22.03	23.74	21.6	16.08	13.87	13.8	23.2
HW	13.4	13.5	15.5	18.6	17.5	17.2	14.69	18.6	14.5	16.13	13.74	11.82	8.19	7.79	16
HD	8.0	7.7	8.9	10.1	10.4	10.05	9.09	10.07	8.1	9.57	8.55	6.07	5.15	5.5	9.21
ED	4.3	4.1	4.9	5.1	6.01	5.52	5.79	6	4.29	4.97	4.31	3.11	3.18	3.32	5.05
EE	5.4	5.8	6.9	8.3	7.7	7.29	6.06	7.1	6.09	7.09	6.41	4.1	3.32	3.32	7.13
ES	7.7	7.6	8.9	10.1	9.5	9.47	8.26	10.4	8.19	8.9	8.51	6.13	4.93	4.98	8.93
EN	6.1	5.9	6.9	7.7	7.5	7.43	6.7	7.6	6.57	6.8	6.21	4.6	3.76	4.01	7.26
IO	5.2	5.2	5.4	6.7	6.9	6.65	5.91	6.6	5.64	6.14	6.11	4.52	3.76	3.18	5.85
EL	2.2	1.5	2.1	2.3	2.2	2.15	1.55	2	2.05	1.33	2.41	1.38	1.18	1.12	2.67
IN	1.8	2.1	2.0	2.7	2.4	2.69	2.25	2.9	2.46	2.73	2.28	1.96	1.31	1.43	2.24

	CAS	CAS	CAS	CAS	CAS	CAS	CAS	CAS	CAS	CAS	CAS	CAS	CAS	CAS
	240335	240414j	240505	240641	240610	240611	240610	240611	240611	240611	240611	240611	240611	240408
Sex	f	J	f	f	f	f	f	f	f	f	f	f	f	f

Supralabials	9	8	9	8	8	8	8	8	8	8	8	8	8	8	8
Infralabials	8	6	7	7	7	7	7	7	7	7	7	7	7	7	7
Body tubercles low, weakly keeled	no	YES	no												
Body tubercles raised, moderately to strongly keeled	yes	no	yes												
Paravertebral tubercles	30	31	32	32	32	32	32	32	32	32	32	32	31	32	32
Longitudinal rows of body tubercles	19	19	20	19	20	19	20	19	19	19	21	18	18	21	21
Tubercles extend beyond base of tail	/	yes													
Ventral scales	31	27	25	25	25	25	25	25	25	25	25	25	25	25	25
Expanded subdigital lamellae on 4th toe	10	9	9	9	9	9	9	9	9	9	8	9	9	8	8
Unmodified subdigital lamellae on 4th toe	15	15	15	15	15	15	15	15	15	15	15	14	14	13	13
Total subdigital lamellae on 4th toe	25	24	24	24	24	24	24	24	24	24	23	23	23	21	21
Enlarged femoral scales (R/L)	15/15	13/13	13/13	13/13	13/13	13/12	12/12	12/12	13/12	13/12	12/12	13/12	13/12	13/13	13/13
Total femoral scales	30	26	26	26	26	25	26	26	25	24	24	25	25	26	26
Femoral pores (R/L)	/	/	/	/	/	/	/	/	/	/	/	/	/	/	/
Total femoral pores in males	/	/	/	/	/	/	/	/	/	/	/	/	/	/	/
Enlarged Precolocal scales	8	9	9	9	9	9	9	9	9	10	10	10	10	9	9
Precolocal pores	/	/	/	/	/	/	/	/	/	/	/	/	/	/	/
Post-precolocal scales rows	3	3	3	3	3	3	3	3	3	3	3	3	3	3	3
Enlarged femoral and precolocal scales continuous	yes														
Pore-bearing femoral and precolocal scales continuous	/	/	/	/	/	/	/	/	/	/	/	/	/	/	/
Enlarged proximal femoral scales ~1/2 size of distal femorals	no	yes	no												
Medial subcaudals 2 or 3 times wider than long	/	yes													
Medial subcaudals extend onto lateral surface of tail	/	no													
SVL	88.51	35.83	82.13	83.31	83.31	83.31	83.31	83.31	83.31	83.31	74.97	85.67	85.67	84.88	84.88
TL	/	/	/	/	/	/	/	/	/	/	/	/	/	/	/
FL	12.93	5.86	13.72	13.59	13.59	13.59	13.59	13.59	13.59	13.59	11.52	13.6	13.6	13.36	13.36
TBL	17.63	7.15	15.84	16.99	16.99	16.99	16.99	16.99	16.99	16.99	16.15	16.97	16.97	15.25	15.25

Sex	CAS											
	f	J	f	J	f	J	f	J	f	J	f	J
AG	35.68	14.8	35.37	14.8	31.14	14.8	31.37	14.8	35.87	14.8	36.67	14.8
HL	26.37	11.99	24.68	11.99	23.47	11.99	22.69	11.99	24.89	11.99	24.68	11.99
HW	18.06	6.71	15.68	6.71	15.75	6.71	14.32	6.71	16.58	6.71	16.15	6.71
HD	10.29	4.28	9.84	4.28	9.41	4.28	8.85	4.28	10.06	4.28	9.98	4.28
ED	6.47	3.33	5.74	3.33	6.66	3.33	6.02	3.33	5.59	3.33	5.5	3.33
EE	8.45	3.56	7.99	3.56	7.72	3.56	6.7	3.56	7.16	3.56	7.22	3.56
ES	10.93	3.75	10.38	3.75	9.99	3.75	8.59	3.75	10.06	3.75	10.97	3.75
EN	8.51	3.21	7.31	3.21	7.35	3.21	6.57	3.21	7.88	3.21	9.29	3.21
IO	7.87	3.05	7.46	3.05	7.37	3.05	5.13	3.05	6.43	3.05	5.57	3.05
EL	2.15	1.35	2.11	1.35	2	1.35	1.56	1.35	2.24	1.35	2.03	1.35
IN	2.6	1.19	2.54	1.19	2.67	1.19	2.26	1.19	2.38	1.19	2.5	1.19

Table A3. Meristic and mensural data from the Kou Thi Nar Youn population of *Cyrtodactylus aequalis*. R = right, L = left, / = data unobtainable or not applicable, r = regenerated.

	LSUHC										
	14491	14492	14493	14494	14495	14496	14497	14498	14499	14500	14501
Sex	M	M	F	M	M	M	F	M	F	F	M
Supralabials	8	8	8	8	8	8	9	8	7	8	8
Infralabials	7	7	7	7	7	7	7	7	6	7	7
Body tubercles low, weakly keeled	no										
Body tubercles raised, moderately to strongly keeled	yes										
Paravertebral tubercles	35	33	32	32	31	31	32	31	32	32	31
Longitudinal rows of body tubercles	19	19	20	20	19	20	20	20	20	18	18
Tubercles extend beyond base of tail	/	yes									
Ventral scales	22	26	23	26	25	25	23	24	27	27	25
Modified subdigital lamellae on 4th toe	8	8	8	8	8	8	8	9	9	9	9
Unmodified subdigital lamellae on 4th toe	16	15	15	15	15	13	14	13	15	15	14
Total subdigital lamellae on 4th toe	24	23	23	23	23	21	22	22	24	24	23
Enlarged femoral scales (R/L)	13/14	14/15	13/13	13/13	14/14	14/14	12/12	13/14	13/14	13/14	13/13
Total femoral scales	27	29	26	26	28	28	24	27	27	27	26
Femoral pores (R/L)	7/8	7/8	/	8/8	6/6	6/6	/	8/7	/	/	7/7
Total femoral pores in males	15	15	/	16	12	12	/	15	/	/	14
Enlarged Preloacal scales	10	10	9	9	10	8	9	10	10	9	9
Preloacal pores	10	10	/	9	7	8	/	10	/	/	9
Post-preloacal scales	3	3	3	3	3	3	3	3	3	3	3
Enlarged femoral and preloacal scales continuous	yes										
Pore-bearing femoral and preloacal scales continuous	no	no	/	no	no	no	/	no	/	/	no
Enlarged proximal femoral scales ~1/2 size of distal femorals	no										
Medial subcaudals 2 or 3 times wider than long	/	yes									
Medial subcaudals extend onto lateral surface of tail	/	no									
SVL	88.8	86.62	75.79	75.25	69.43	68.48	71.03	67.63	64.32	78.50	67.97
FL	12.94	14.69	11.64	12.46	10.42	10.73	9.82	10.16	9.87	11.63	10.91
TBL	16.4	16.57	14.46	15.61	13.41	13.73	12.95	12.65	11.85	14.73	13.75
AG	37.55	36.39	34.82	33.44	31.1	28.35	34.58	30.22	28.56	35.32	29.04
HL	25.51	25.8	21.93	21.84	20.34	19.91	20.77	22.08	18.18	23	20.12
HW	16.92	18.06	14.45	14.69	13.84	13.29	13.69	12.9	12.68	15.02	12.83
HD	10.46	10.16	8.23	8.68	8.25	7.69	7.93	7.76	6.82	8.76	7.82
ED	6.11	6.33	5.66	5.29	4.81	4.06	4.49	5.04	5.02	4.73	4.36
EE	7.49	6.96	6.31	6.24	5.64	5.34	5.69	6.06	5.29	6.24	5.28
ES	10.67	10.2	8.41	9.32	8.47	7.64	8.3	8.14	7.74	9.27	7.07
EN	7.53	7.08	5.41	6.57	5.94	6.31	5.73	6.03	5.49	6.26	5.88
IO	7.68	6.19	5.9	4.78	4.98	4.55	5.83	5.81	5.14	6.65	4.45
EL	2.09	2.29	1.48	1.85	1.63	2.17	1.78	2.49	1.46	1.73	2.18
IN	2.73	2.65	2.33	2.44	1.81	2.15	2.18	2.18	1.95	2.82	1.7

Table A4. Summary statistics of the three allopatric populations of *Cyrtodactylus aequalis*. SD = standard deviation, n = sample size, and * and # denote significant statistical differences between specified means.

	Kyaiktiyo	Kay Lar Tha	Kou Thi Nar Youn
supralabial scales (SL)			
mean (\pm SD)	8.2 (\pm 0.50)	8.0 (\pm 0.00)	8.0 (\pm 0.45)
range	7–9	8	7–9
n	22	4	11
infralabial scales (IL)			
mean (\pm SD)	6.5 (\pm 0.60)	6.75 (\pm 0.50)	6.9 (\pm 0.30)
range	6–8	6 or 7	6 or 7
n	22	4	11
paravertebral tubercles (PT)			
mean (\pm SD)	*32.6 (\pm 1.37)	*#29.0 (\pm 0.00)	#32.0 (\pm 0.18)
range	30–35	29	31–35
n	22	4	11
longitudinal rows of body tubercles (LT)			
Mean (\pm SD)	*21.1(\pm 1.42)	20.8 (\pm 0.50)	*19.4 (\pm 0.81)
Range	18–23	20 or 21	18–20
n	22	4	11
ventral scales (VS)			
mean (\pm SD)	24.4 (\pm 1.84)	24.5 (\pm 0.58)	24.8 (\pm 1.67)
range	22–31	24 or 25	22–27
n	22	4	11
expanded 4th toe lamellae (ETL)			
mean (\pm SD)	*8.8 (\pm 0.73)	*7.5 (\pm 0.58)	8.4 (\pm 0.50)
range	7–10	7 or 8	8 or 9
n	22	4	11
unmodified 4th toe lamellae (UTL)			
mean (\pm SD)	14.2 (\pm 0.97)	15.0 (\pm 1.41)	14.5(\pm 0.93)
range	13–17	13–16	13–16
n	22	4	11
total 4th toe lamellae (TTL)			
mean (\pm SD)	23.0 (\pm 0.90)	22.5 (\pm 1.29)	22.9(\pm 0.94)
range	21–25	21–24	21–24
n	22	4	11
enlarged femoral scales (FS)			
mean (\pm SD)	*24.9 (\pm 1.81)	#24.5 (\pm 1.29)	*#26.8 (\pm 1.33)
range	22–30	23–26	24–29
n	22	4	11
femoral pores (FP)			
mean (\pm SD)	14.4 (\pm 2.94)	/	14.1(\pm 0.57)
range	10–19	/	12–16
n	7	/	7
enlarged precloacal scales (PS)			
mean (\pm SD)	9.0 (\pm 0.84)	8.8 (\pm 0.50)	9.4 (\pm 0.67)
range	7–10	8 or 9	8–10
n	22	4	11
precloacal pores (PP)			
mean (\pm SD)	7.4 (\pm 2.07)	/	9.0(\pm 0.15)
range	5–10	/	7–10
n	7	/	7
post-precloacal scale rows (PPS)			
mean (\pm SD)	3.0 (\pm 0.00)	3.0 (\pm 0.00)	3.0 (\pm 0.00)
range	3	3	3
n	22	4	11
maximum SVL (mm)	99.0	74.0	88.8
n	22	4	11

Table A5. Uncorrected pairwise sequence divergences between the mitochondrial ND2 lineages of the *Cyrtodactylus aequalis* populations.

	2	3	4	5	6	7	8	9	10	11	12	13	14	15	16
2. LSUHC 14052 Kyaikto															
3. LSUHC 14053 Kyaikto	0.004														
4. LSUHC 14054 Kyaikto	0.003	0.001													
5. LSUHC 14055 Kyaikto	0.001	0.003	0.002												
6. LSUHC 14056 Kyaikto	0.003	0.001	0.000	0.002											
7. LSUHC 14057 Kyaikto	0.000	0.004	0.003	0.001	0.003										
8. LSUHC 14058 Kyaikto	0.003	0.001	0.000	0.002	0.000	0.003									
9. LSUHC 14059 Kyaikto	0.003	0.001	0.000	0.002	0.000	0.003	0.000								
10. LSUHC 14060 Kyaikto	0.003	0.005	0.004	0.002	0.004	0.003	0.004	0.004							
11. LSUHC 14061 Kyaikto	0.001	0.003	0.002	0.000	0.002	0.001	0.002	0.002	0.002						
12. LSUHC 14062 Kyaikto	0.001	0.004	0.003	0.001	0.003	0.001	0.003	0.003	0.003	0.001					
13. LSUHC 14063 Kyaikto	0.001	0.004	0.003	0.001	0.003	0.001	0.003	0.003	0.003	0.001	0.001				
14. LSUHC 14064 Kyaikto	0.001	0.003	0.002	0.000	0.002	0.001	0.002	0.002	0.002	0.000	0.001	0.001			
15. LSUHC 14065 Kyaikto	0.001	0.004	0.003	0.001	0.003	0.001	0.003	0.003	0.003	0.001	0.001	0.001	0.001		
16. LSUHC 12895 Kyaikto	0.003	0.004	0.004	0.002	0.004	0.003	0.004	0.004	0.004	0.002	0.002	0.003	0.002	0.003	
17. LSUHC 14491 Kou Thi Nar	0.004	0.005	0.004	0.004	0.004	0.004	0.004	0.004	0.006	0.004	0.004	0.004	0.004	0.004	0.004
18. LSUHC 14492 Kou Thi Nar	0.002	0.003	0.002	0.001	0.002	0.002	0.002	0.002	0.004	0.001	0.002	0.002	0.001	0.002	0.003
19. LSUHC 14493 Kou Thi Nar	0.004	0.004	0.004	0.003	0.004	0.004	0.004	0.004	0.005	0.003	0.004	0.004	0.003	0.004	0.004
20. LSUHC 14494 Kou Thi Nar	0.002	0.003	0.002	0.001	0.002	0.002	0.002	0.002	0.004	0.001	0.002	0.002	0.001	0.002	0.003
21. LSUHC 14495 Kou Thi Nar	0.002	0.003	0.002	0.001	0.002	0.002	0.002	0.002	0.004	0.001	0.002	0.002	0.001	0.002	0.003
22. LSUHC 14496 Kou Thi Nar	0.002	0.003	0.002	0.001	0.002	0.002	0.002	0.002	0.004	0.001	0.002	0.002	0.001	0.002	0.003
23. LSUHC 14497 Kou Thi Nar	0.005	0.006	0.005	0.004	0.005	0.005	0.005	0.005	0.007	0.004	0.005	0.005	0.004	0.005	0.006
24. LSUHC 14498 Kou Thi Nar	0.002	0.003	0.002	0.001	0.002	0.002	0.002	0.002	0.004	0.001	0.002	0.002	0.001	0.002	0.003
25. LSUHC 14499 Kou Thi Nar	0.005	0.004	0.004	0.004	0.004	0.005	0.004	0.004	0.007	0.004	0.005	0.004	0.004	0.004	0.008
26. LSUHC 14500 Kou Thi Nar	0.007	0.005	0.005	0.005	0.005	0.007	0.005	0.005	0.008	0.005	0.007	0.005	0.005	0.005	0.008
27. LSUHC 14501 Kou Thi Nar	0.004	0.004	0.004	0.003	0.004	0.004	0.004	0.004	0.004	0.003	0.004	0.004	0.003	0.004	0.003
28. LSUHC 14242 Kay Lar Tha	0.012	0.013	0.012	0.012	0.012	0.012	0.012	0.012	0.014	0.011	0.012	0.012	0.012	0.012	0.013
29. LSUHC 14243 Kay Lar Tha	0.012	0.013	0.012	0.012	0.012	0.012	0.012	0.012	0.014	0.012	0.012	0.012	0.012	0.012	0.013
30. LSUHC 14244 Kay Lar Tha	0.012	0.013	0.012	0.012	0.012	0.012	0.012	0.012	0.014	0.011	0.012	0.012	0.012	0.012	0.013
31. LSUHC 14245 Kay Lar Tha	0.012	0.013	0.012	0.012	0.012	0.012	0.012	0.012	0.014	0.012	0.012	0.012	0.012	0.012	0.013
32. LSUHC 14491 Kou Thi Nar	0.004	0.004	0.004	0.004	0.004	0.004	0.004	0.004	0.004	0.004	0.004	0.004	0.004	0.004	0.004
Youn	17	18	19	20	21	22	23	24	25	26	27	28	29	30	31

	2	3	4	5	6	7	8	9	10	11	12	13	14	15	16
33. LSUHC 14492 Kou Thi Nar Youn	0.003	0.002													
34. LSUHC 14493 Kou Thi Nar Youn	0.004	0.004	0.001												
35. LSUHC 14494 Kou Thi Nar Youn	0.003	0.002	0.000	0.001											
36. LSUHC 14495 Kou Thi Nar Youn	0.003	0.002	0.000	0.001	0.000										
37. LSUHC 14496 Kou Thi Nar Youn	0.003	0.002	0.000	0.001	0.000	0.000									
38. LSUHC 14497 Kou Thi Nar Youn	0.006	0.005	0.003	0.001	0.003	0.003	0.003								
39. LSUHC 14498 Kou Thi Nar Youn	0.003	0.002	0.000	0.001	0.000	0.000	0.000	0.003							
40. LSUHC 14499 Kou Thi Nar Youn	0.008	0.004	0.001	0.001	0.001	0.001	0.001	0.001	0.001	0.001	0.001				